1262148

Geologic Framework

By Douglas B. Yager and Dana J. Bove

Chapter E1 of

Integrated Investigations of Environmental Effects of Historical Mining in the Animas River Watershed, San Juan County, Colorado

Edited by Stanley E. Church, Paul von Guerard, and Susan E. Finger

Professional Paper 1651

U.S. Department of the Interior
U.S. Geological Survey

Contents

Abstract 111
Introduction 112
Geographic Setting 112
Previous Geologic Investigations 113
Regional Tectonic Setting 113
Pre-Oligocene Rocks of the Animas River Watershed Study Area and Vicinity 115
- Precambrian Rocks 115
- Paleozoic Rocks 117
- Mesozoic Rocks 117
- Tertiary Sedimentary Rocks 119

Mid-Tertiary Volcanic Rocks 121
- Precaldera Rocks 121
- San Juan–Uncompahgre Caldera and Silverton Caldera Rocks 121

Tertiary Structures and Veins of the San Juan–Uncompahgre and Silverton Calderas 126
- Caldera Ring Faults 126
- San Juan Caldera Topographic Margin 126
- Eureka Graben Faults and Formation of Radial Fracture Pattern 127
- Mineralized Faults and Fractures 128
- Implications of Caldera Faults and Veins as Flow Paths 130

Alteration Types 130
- Regional Propylitic Alteration 130
- Weak Sericite-Pyrite Alteration 133
- Vein-Related Quartz-Sericite-Pyrite Alteration 133
- Quartz-Sericite-Pyrite Alteration 133
- Acid-Sulfate Alteration 133

Acid-Generating Capacity of Non-Mining-Affected Rocks 133
Acid-Neutralizing Capacity of Study Area Rocks 133
- Metamorphic Rock Acid-Neutralizing Capacity 133
- Sedimentary Rock Acid-Neutralizing Capacity 134
- Tertiary Volcanic Rock Acid-Neutralizing Capacity 134
- Surficial Deposit Acid-Neutralizing Capacity 135

Late Tertiary Erosion 135
Glaciation Events 135
Pleistocene to Holocene Fluvial Geomorphologic Conditions 136
Summary 136
References Cited 137

Plates

[Plates in this report are on accompanying CD-ROM]

1. Generalized geologic map of part of the Animas River watershed and vicinity, Silverton, Colorado
2. Ferricrete, manganocrete, and bog iron occurrences with selected sedge bogs and active iron bogs and springs in part of the Animas River watershed, San Juan County, Colorado

Figures

1. Regional tectonic map of southwest Colorado and northwest New Mexico.....114
2. Generalized regional geologic map of Animas River watershed study area 116
3. Stratigraphic column for rocks in Animas River watershed study area 118
4. Map showing geographic feature names and mining districts in Animas River watershed study area 120
5. Diagrams showing total alkali versus silica classification.....122
6. Regional map showing calderas of San Juan volcanic field and generalized rock types.....123

7–9. Diagrams showing:
   7. Total alkali versus silica, alkaline-subalkaline classification.....124
   8. Potassium versus silica classification.....124
   9. Strontium versus silica classification 125

10. Total alkali, total iron and magnesium ternary diagram showing calc-alkaline and tholeiitic classification fields 126
11. Photograph of fractured and mineralized Silverton caldera structural margin along Mineral Creek.....127
12. Landsat image showing erosion along structural margin of Silverton caldera by Mineral Creek and Animas River 128
13. Generalized north-south cross section across Silverton caldera structural margin.....129
14. Generalized alteration map of Animas River watershed study area 131
15. Photomicrographs of propylitized intermediate-composition volcanic rocks 132
16. Photomicrograph of calcite and chlorite microveinlet in intermediate-composition Silverton Volcanics lava flow.....134

Tables

1. Major vein minerals of the Sunnyside mine workings 130
2. Minor (<0.5 volume percent) vein minerals of the Sunnyside mine workings.....130

Chapter E1
Geologic Framework

By Douglas B. Yager and Dana J. Bove

Abstract

This geologic summary and accompanying maps of part of the Animas River watershed, western San Juan Mountains, Colorado, provide a basic geologic framework for this volume. The Animas River headwater region of this volume consists of a Precambrian crystalline basement overlain by Paleozoic and Mesozoic sedimentary rocks and by a Tertiary volcanic cover.

The Tertiary is marked by deposition of the Eocene Telluride Conglomerate on an extensively eroded Eocene surface. The Telluride Conglomerate is host to Oligocene to Miocene polymetallic replacement mineral deposits. A sequence of Tertiary volcanic rocks overlying the Telluride Conglomerate comprises the majority of rocks exposed in the Animas River watershed study area. Tertiary volcanism commenced in the study area about 35 million years ago with the eruption of intermediate-composition lava flows and deposition of volcaniclastic mudflow deposits of the San Juan Formation. Caldera-related volcanism began shortly after the early San Juan Formation volcanism ceased, with the formation of the 28.2 Ma San Juan caldera, source of the Sapinero Mesa Tuff, and nearly contemporaneous Uncompahgre caldera, source of the Dillon Mesa Tuff. Post-caldera collapse volcanism consisted of lower Silverton Volcanics intermediate-composition lava flows and volcaniclastic rocks that filled the San Juan caldera. An elliptical dome formed between the San Juan and Uncompahgre calderas, and extensional fracturing over the resurgent dome of the intracaldera fill resulted in Eureka graben formation. Faults of the Eureka graben were extensively mineralized, primarily within the intermediate-composition Silverton Volcanics lavas. The Silverton caldera collapsed in response to eruption of the Crystal Lake Tuff at 27.6 Ma and is nested within the older San Juan caldera.

The San Juan–Uncompahgre and Silverton calderas are characterized by an extensive system of faults and veins. A highly fractured, arcuate, caldera ring fault zone is exposed along parts of Mineral Creek and along the Animas River southeast of Silverton. Radial faults that are tangential to the ring fault zone formed in response to broad resurgence that affected a region extending well beyond the San Juan caldera margin. The northwest-trending radial faults are apparently more highly mineralized when compared with radial faults with other orientations or with caldera ring faults. Resurgent doming within the central core of the San Juan–Uncompahgre calderas also resulted in the formation of a northeast-trending graben that was extensively mineralized. The primary host for base metals and precious metals in the study area is the intermediate-composition Silverton Volcanics lavas, where this unit is cut by graben-related and radial structures. Faults associated with the San Juan–Uncompahgre calderas localized post-Silverton-caldera, late-stage dacitic to rhyolitic intrusions and associated post-caldera hydrothermal mineralizing fluids that leached acid-neutralizing bedrock. These faults may be possible ground-water flow paths for trace-element- and major-element-rich water.

Five general alteration types formed in response to hydrothermal alteration events, which affected the Animas River watershed study area and followed caldera formation by 1 million to several million years. The five alteration types, listed in increasing order of intensity, are regional propylitic alteration, weak sericite-pyrite alteration, vein-related quartz-sericite-pyrite alteration, quartz-sericite-pyrite alteration, and acid-sulfate alteration. The propylitic alteration event, which affected most if not all volcanic rocks in the study area, introduced the assemblage of quartz-epidote-chlorite-calcite-pyrite-iron oxides. Locally, volcanic rocks were overprinted with higher grades of alteration. The incidence of sericite along with the propylitic assemblage is recognized in areas of densely spaced veins and adjacent to areas of the more intensely altered quartz-sericite-pyrite assemblage. The quartz-sericite-pyrite assemblage is indicative of more intensely altered areas that formed closer to a hydrothermal heat source and is characterized by the primary minerals of the original host rock being altered to a fine-grained rock of quartz, sericite, and pyrite. The most intense alteration, the acid-sulfate assemblage, is characterized by the mineral assemblages of quartz-alunite and (or) quartz-pyrophyllite, with some argillic alteration zones.

Many of the geologic units contain primary and secondary mineral assemblages that have some limited potential to mitigate acidic drainage from mine sites or unmined mineralized rocks. A host rock or surficial deposit that contains calcium carbonate, or the assemblage chlorite-calcite-epidote, has a high acid-neutralizing capacity. The neutralizing

capacity of rocks locally, and in some cases over large subbasin areas, is limited because intense hydrothermal alteration associated with mid- to late-Tertiary volcanism has replaced acid-neutralizing mineral assemblages with acid-generating sulfide minerals. Rocks that have high acid-neutralizing mineral assemblages in the Animas River watershed include Precambrian amphibolites, schists, and gneisses with the chlorite-epidote-calcite assemblage, and Paleozoic and Mesozoic limestones, dolomites, mudstones, and calcareous sandstones. Among the Tertiary sedimentary rocks, the Telluride Conglomerate locally contains limestone clasts. The younger Silverton Volcanics lavas are voluminous and extensively propylitized to calcite, chlorite, and epidote; within the study area, this unit likely has the most significantly high acid-neutralizing capacity, where it is not intensely altered by hydrothermal mineralization events. Weathering of bedrock in headwater subbasins has resulted in deposition of surficial deposits. Quaternary surficial deposits provide ground-water flow paths throughout as much as 27 percent of the headwater regions of the Animas River watershed study area, which facilitate water-rock interaction when infiltrated by ground water. The surficial deposits are acid generating or acid neutralizing depending on the mineralogic assemblages from which they were eroded.

During the late Miocene to Pliocene, when the San Juan Mountains were differentially uplifted relative to the Rio Grande Rift basin to the southeast, accelerated weathering and erosion exposed volcanogenic sulfides to surface water and ground water and increased acid drainage in the Animas River watershed. Pleistocene glaciation scoured the region, further exposing mineralized bedrock to weathering. During the height of the Wisconsin glaciation, a 1-km thick ice sheet covered 20 percent of the western San Juan Mountains. Easily erodable cirque basins with oversteepened slopes were exposed after glacier retreat.

Ferricrete, which consists of surficial deposits cemented in place by iron oxyhydroxide, occurs throughout the watershed study area. The surficial deposits serve as flow paths and precipitation sites for iron-rich water derived from the oxidation of pyrite. They are an indicator of acidic conditions that have existed in the watershed before, during, and after mining.

Introduction

This chapter and the geologic map (pl. 1) summarize the geologic setting for the Animas River watershed study area and provide a geologic framework for assessing acid rock drainage issues in the reports that follow. The Animas River watershed study area is located in the western San Juan Mountains near Silverton, Colo. This chapter includes discussions of

- The tectonic setting of the western San Juan Mountains
- Principal rock types in the study area and vicinity with mention of the lithologies that have a high acid-neutralizing capacity
- Caldera-related structures that are potential ground-water flow paths
- Major alteration types
- Late Tertiary erosion events and Pleistocene glaciation, which have exposed bedrock to weathering.

The elements of the geologic map (pl. 1) that are important to the study include

- Numerous rock types, wherein chemical constituents of minerals that compose the rocks interact with surface water and ground water and affect water quality
- Igneous bedrock units that are hosts for Tertiary mineralization and are locally intensely altered and regionally weakly altered
- Distribution of the caldera-related veins, which have been extensively mined for base-metal sulfides and precious metals
- Distribution of permeable surficial deposits that are conduits for shallow ground water systems.

The Animas River watershed study area is located in the western part of the San Juan volcanic field, which is one of the largest erosional remnants of a volcanic province that covers much of the southern Rocky Mountain region (Steven and Epis, 1968; Steven, 1975). Of great importance to the Animas River watershed geologic history are the volcanotectonic and mineralization events that occurred from 35 to 10 Ma. Sulfide minerals that formed during mineralization events between 22 and 10 Ma, where exposed by weathering and erosion or by mining, have generated acid water and introduced major elements and trace elements to surface water. Tertiary-age mineralized fault zones and veins were extensively mined in this region from the late 19th century through most of the 20th century (Bove and others, this volume, Chapter E3; Nash and Fey, this volume, Chapter E6), which exposed the sulfide system to weathering.

Geographic Setting

A discussion of the geographic setting is important in a geologic context, because geography strongly influences the geoenvironmental weathering processes affecting the watershed. The western San Juan Mountains are rugged and steep, their terrain further emphasized by Pleistocene glaciation and Holocene erosion. Topographic relief in the study area reaches 1,000 m with a maximum elevation exceeding 4,000 m above sea level. Precipitation, falling mainly as snow during the fall, winter, and spring seasons, is as much as 60 cm (Gillam, 1998). Snowmelt is strongly controlled by slope and aspect (orientation in relation to the sun's azimuth), in addition to time of year and elevation. On steep north-facing slopes,

snow remains even in the summer and fall months, following a winter with normal precipitation. In contrast, south-facing slopes that receive direct sunlight are usually snow free from late spring to early fall. Thus, the volume of acid rock drainage will vary for each subbasin throughout the year, which in turn will influence the rate and amount of water-rock interaction. Mean annual ambient air temperature in the study area is approximately 2°C (Gillam, 1998). Bedrock is subject to strong mechanical weathering by exposure to frequent freeze-thaw temperature fluctuations, which in turn expose freshly broken surfaces to continued water-rock interaction (Hoch and others, 1999).

The western San Juan volcanic field is part of the Southern Rocky Mountain steppe ecoregion (Bailey, 1995). Only sparsely vegetated alpine zone tundra is present at high elevation. Where altered bedrock and steep slopes coincide, the fragile vegetation patterns cannot stabilize the easily erodable outcrops, which constantly contribute mineral-laden sediment to streams below them. The subalpine zone is delimited by Engelmann spruce and subalpine fir. At lower elevations, riparian vegetation consists of grasses, sedge grasses, mosses, and willows.

Previous Geologic Investigations

The Animas River watershed investigations follow the work of past geologists whose focus and scope of study have evolved over a 130-year period to meet changing scientific and social needs. The discovery and exploitation of economically important base and precious metals in the northern part of the Animas River watershed during the 1870s spawned early geologic investigations. Today, we are interested in the combined effect that weathering both of altered and mineralized bedrock and of mine waste has on water quality and aquatic ecosystems.

Early investigators attempted to decipher the general stratigraphy and mineral deposits of the area near Silverton, Colo. (Ransome, 1901; Cross and others, 1905). These works were the foundation for later descriptions of the regional aspects of ore deposits in the San Juan Mountains (Burbank and Luedke, 1968; Steven and others, 1969). Focused mineral deposit studies were accomplished in the highly profitable Eureka mining district (Burbank and Luedke, 1969; Casadevall and Ohmoto, 1977). Reports and maps of a more general nature that include information on the geologic history and regional stratigraphy of the San Juan Mountains, but which are not referred to in other parts of this chapter, include the works of Kelley (1946), Larsen and Cross (1956), and Steven and others (1974).

The Tertiary volcanotectonic history of the region is the emphasis of several reports. Caldera-related research in the western San Juan Mountains was initiated in the 1960s (Luedke and Burbank, 1968) and has continued as geologists have further refined their concepts about how the San Juan volcanic field has evolved (Ratté and Steven, 1967; Smith and Bailey, 1968; Lipman, 1976a,b; Steven and Lipman, 1976; Lipman, 1984, 2000). Isotopic dating of rocks in and near the Animas River watershed study area has aided in understanding the timing of volcanism in relation to ore deposition (Lipman and others, 1970; Lipman and others, 1976; Bove and others, 2001). The volcanic stratigraphy is discussed in Lipman and others (1973) and Lipman (1976b), and better constrained by isotopic dating (Bove and others, 2001).

Interpretations of the Quaternary glacial history and physiography of the western San Juan Mountains were first provided in the classic work of Atwood and Mather (1932). Modern interpretations of the late Cenozoic geologic history of the region involve discussions of Pleistocene glaciation and variables that have influenced stream terrace formation near Durango, Colo. (Gillam, 1998).

Regional Tectonic Setting

The western San Juan Mountains are situated near the eastern margin of the Colorado Plateau. The Colorado Plateau is a broad region of the southwestern United States that is bordered on the west by the Basin and Range province in Utah and Nevada, on the north by the east-west-trending Uinta uplift of Utah, on the east by the southern Rocky Mountains of Colorado and New Mexico, and on the south by the Mogollon Rim of Arizona.

Southwest Colorado and the western San Juan Mountains have undergone several periods of deformation that date back to the Precambrian. Evidence for two major cycles of Precambrian deposition, folding, metamorphism, and pluton emplacement are recorded in the geologic record of the Precambrian rocks of the Needle Mountains uplift that borders the southern part of the Animas River watershed study area. The first cycle of deposition, metamorphism, and intrusion occurred between 1,800 and 1,700 Ma; the second cycle occurred between 1,650 and 1,450 Ma (Barker, 1969). Intense, generally north to northeast trending folding accompanied the first Precambrian cycle, whereas isoclinal folding to the east and southeast occurred during the second cycle (Barker, 1969). Continental-scale northwest-striking faults formed in the San Juan Mountains at about 1,600 Ma (Baars and Ellingson, 1984). These northwest-trending faults bound Precambrian blocks of the Grenadier Range, located south of Silverton, and the Sneffels horst, located in the vicinity of Ouray (fig. 1). An apparent conjugate set of northeast-striking faults that demarcate the Colorado mineral belt appear to offset the northwest-striking faults (Baars and Ellingson, 1984). The Precambrian basement faults were rejuvenated periodically through the Laramide.

In addition to the major tectonic events, there were at least four episodes of Precambrian intrusive events. The effects of Precambrian intrusions, tumescence, and subsequent erosion continued into the Cambrian (Barker, 1969). The source rocks for the Cambrian Ignacio Quartzite are Precambrian

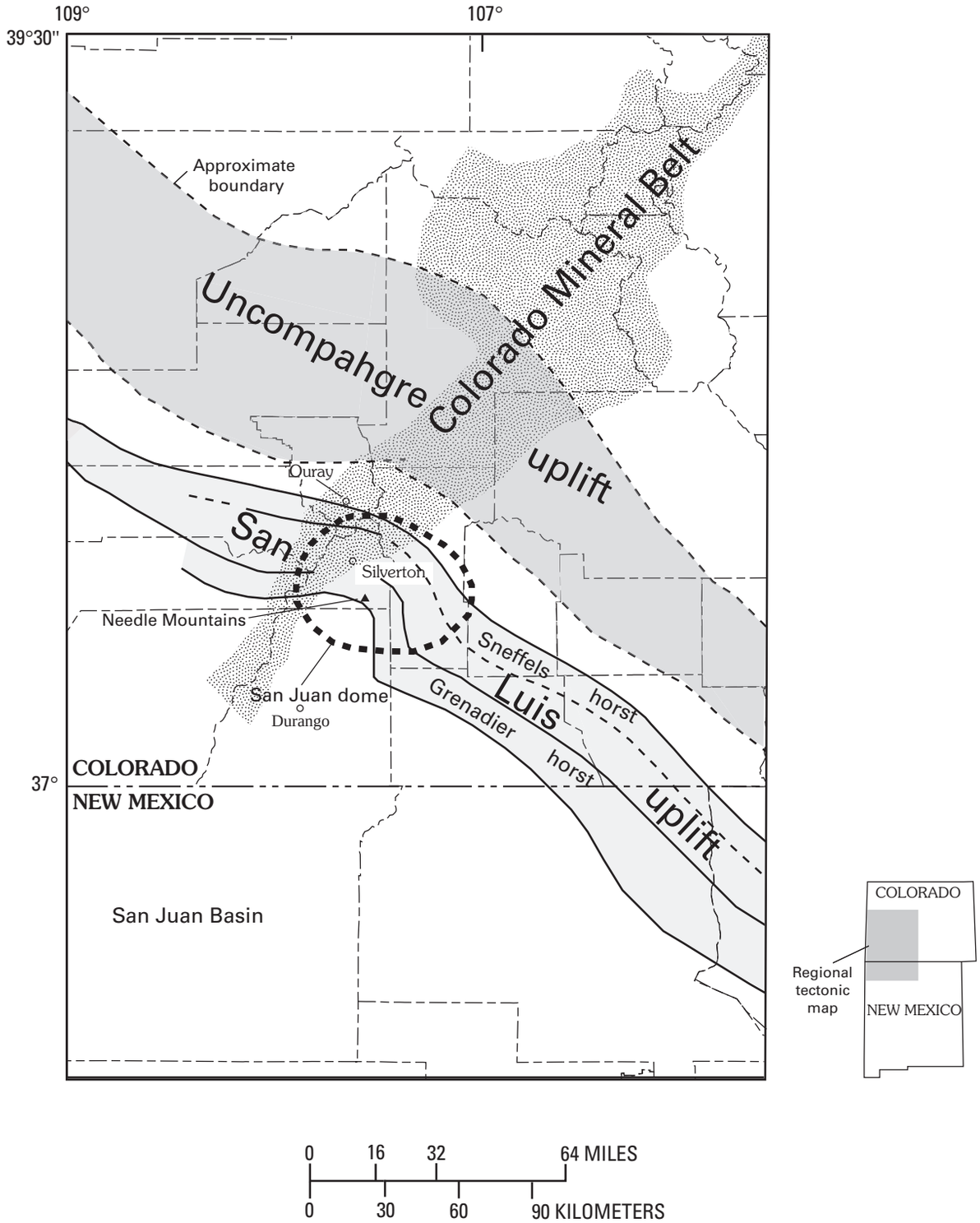

Figure 1. Regional tectonic map of southwest Colorado and northwest New Mexico. Structures bounding Sneffels and Grenadier horsts have been periodically reactivated since the Precambrian. Quartz-rich sediments were shed from horst of San Luis uplift from Cambrian to Pennsylvanian, whereas Uncompahgre uplift was a source of feldspathic sediments to western San Juan Mountains in the Pennsylvanian. The Laramide, broad domal uplift "San Juan dome" is centered near Needle Mountains south of Silverton. Approximate region of Colorado mineral belt (COMB) modified from Tweto and Sims (1963), shown in a stippled pattern. Current political county boundaries are provided as frame of reference. Modified from Baars and Ellingson (1984).

crystalline rocks that were shed from the northwest-southeast-trending Grenadier and Sneffels horst blocks (fig. 1) (Baars and Ellingson, 1984), which were uplifted high above sea level during the Late Cambrian and supplied coarse material to their flanks.

A major mountain-building episode that affected the San Juan Mountains is associated with the Pennsylvanian to Permian San Luis–Uncompahgre uplifts (fig. 1) and formation of the Ancestral Rockies. Late Paleozoic cratonic deformation in western North America in Pennsylvanian time is attributed to the Ouachita-Marathon orogeny, which was likely caused by the collision of South America and Africa with the south edge of the North American landmass (Kluth and Coney, 1981). Fault blocks that bound the Grenadier and Sneffels horst were reactivated and uplifted during the Early Pennsylvanian. These uplifted blocks were sources for quartzose sediments that were deposited in the Ignacio Quartzite, the oldest Paleozoic unit in the study area. Uplift and erosion of the San Luis highland are recorded in deposition of Pennsylvanian Hermosa Formation quartzose sediments, whereas the source of Permian-age Cutler Formation arkosic sediments is the Uncompahgre highland (Baars and Ellingson, 1984). The several blocks of the San Luis–Uncompahgre uplifts were active into the Mesozoic Era and were sediment source areas for the Upper Triassic Dolores Formation, which was unconformably deposited on the Cutler Formation.

Eastward-directed compressive stresses generated during the Laramide orogeny at about 65 Ma were accommodated by Precambrian basement structures (Baars and Ellingson, 1984). This orogeny is inferred to have resulted from east-northeast-directed compression caused by west-southwest convergence of the North American and Farallon plates across the newly rifted North Atlantic (Chapin and Cather, 1981). A relatively symmetrical, basement-cored domal uplift referred to as the "San Juan dome" attained its present proportions during this time (Baars and Ellingson, 1984) and is roughly centered in an area to the south of Silverton in the Needle Mountains (fig. 1). The uplifted and eroded San Juan dome surface rises from an elevation of about 2,800 m just north of Ouray, to 4,000 m in the area between Silverton and Lake City and to more than 4,600 m in the Needle Mountains. Late Cretaceous intrusive magmatism accompanied the Laramide episode of tectonism in the western San Juan Mountains. Intrusive igneous rocks emplaced during the Laramide consist of granodiorite dikes, sills, laccoliths, and small plugs located west and north of the study area (Varnes, 1963). A period of erosion followed the mountain-building episode of the Laramide orogeny, forming the extensive Eocene erosion surface. The Eocene erosion surface is a vast western North America peneplain that formed following a period of both basement-cored uplifts of the Laramide Rocky Mountains and monoclinal uplifts of the Colorado Plateau (Epis and Chapin, 1975; Chapin and Cather, 1981). The Eocene Telluride Conglomerate was deposited during this time; its source rocks were derived from sediments that were shed from the San Luis uplift east of the study area.

Pre-Oligocene Rocks of the Animas River Watershed Study Area and Vicinity

The western San Juan Mountains preserve a relatively complete geologic record from Precambrian to Cenozoic time. Within the Animas River watershed study area, however, multiple Tertiary volcanotectonic and intrusive events have obliterated much of the geologic record. In general, Animas River watershed study area stratigraphy consists of a Precambrian crystalline basement overlain by Paleozoic, Mesozoic, and Eocene-age sedimentary rocks, and a 1- to 2-km thick, Oligocene- to Miocene-age volcanic cover (generalized in fig. 2; see also pl. 1). Figure 3 is an Animas River watershed stratigraphic column, and figure 4 is an index map for geographic feature names in the watershed.

Precambrian Rocks

In the context of this investigation, the Precambrian rocks are important because they contain mineral phases whose high acid-neutralizing capacity influences water-rock interaction in the south part of the study area, near the headwater region of Cunningham Creek and along the Animas River south of Silverton. Precambrian basement rock structures have also influenced the structural history of the entire San Juan Mountains throughout Paleozoic to Cenozoic time (Tweto and Sims, 1963; Baars and Ellingson, 1984).

Largely due to later Tertiary volcanotectonic events, the Precambrian rocks crop out near the periphery of the Animas River watershed study area—principally along the Animas River downstream of Silverton, near Cunningham Creek, near the eastern margin of the watershed, east of the historical Animas Forks townsite, and north of Abrams Mountain (fig. 4; pl. 1). According to Barker (1969) and Luedke and Burbank (2000), the Precambrian rocks along the Animas River downstream of Silverton and at the headwaters of Cunningham Creek are equivalent to the Irving Formation in the Needle Mountains farther to the south. Irving Formation rocks consist of interlayered fine-grained, dark-gray to greenish-gray banded amphibolite with various fine-grained, gray to green, plagioclase-quartz-biotite-bearing gneisses and minor sericite-biotite-chlorite schists (Barker, 1969). Amphibolite is the predominant rock type in the Irving Formation and consists of blue-green hornblende, calcic oligoclase, and epidote; varieties with biotite, chlorite, and quartz are not uncommon (Barker, 1969). In many places, plagioclase-quartz-biotite-bearing gneisses contain one or more of the following phases: chlorite, epidote, microcline, garnet, calcite, magnetite, and pyrite. Regional uplift, tilting to the west, and subsequent retrograde metamorphism (Steven and others, 1969) resulted in formation and concentration of the acid-neutralizing mineral assemblage of chlorite-epidote-calcite (Desborough and Driscoll, 1998; Desborough and Yager, 2000).

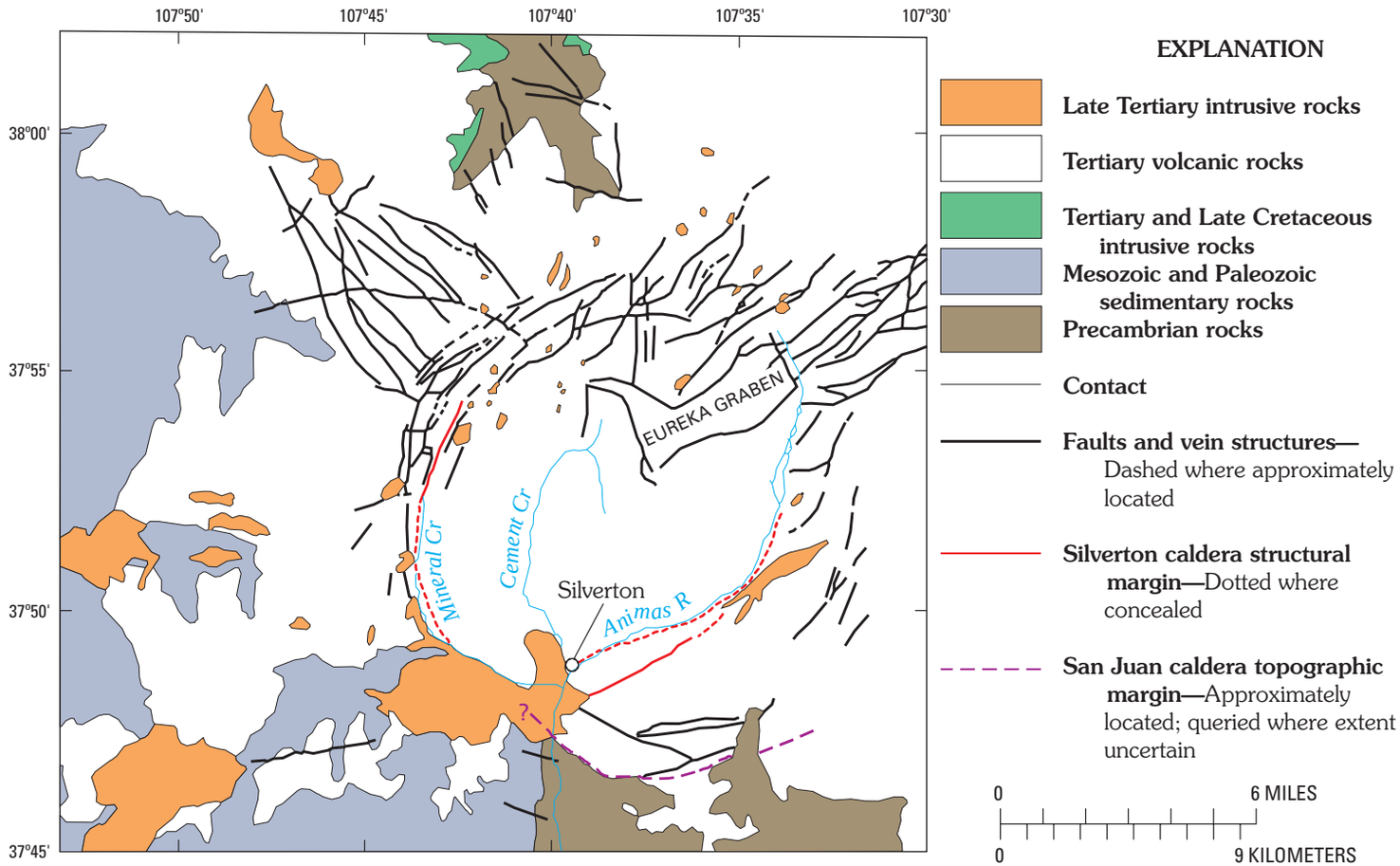

Figure 2. Generalized regional geology of Animas River watershed study area and surrounding regions near Silverton, Colo. Major tributaries to Animas River are shown in addition to major Tertiary volcanotectonic structures related to Silverton and San Juan calderas. Modified from Casadevall and Ohmoto (1977).

Paleozoic Rocks

Paleozoic sedimentary rocks are primarily exposed south of Silverton and generally dip to the west (fig. 2; pl. 1) (Luedke and Burbank, 2000). The thickest outcrops are preserved along the Animas River downstream of Silverton and in the basins draining South Fork Mineral Creek.

The Cambrian Ignacio Quartzite represents the oldest unit of the Paleozoic section. The basal Ignacio Quartzite consists of a quartzite conglomerate, which grades upward to sandstone, siltstone, mudstone, and thinly bedded dolomite (Baars and Ellingson, 1984). Ignacio Quartzite rests unconformably on Precambrian basement along the Animas River downstream of Silverton. Ordovician, Silurian, and Lower and Middle Devonian units are absent from the western San Juan Mountains, probably owing to a combination of nondeposition and a mid-Devonian erosional event (Baars and Ellingson, 1984).

A variable 77-m thick sequence of Upper Devonian Elbert Formation shale and limestone and Upper Devonian Ouray and Mississippian Leadville Limestones overlies the Ignacio Quartzite. The Ouray Limestone is commonly brown, micritic, and dolomitized (Baars and Ellingson, 1984). The overlying cliff-forming Leadville Limestone is locally dolomitized and chemically weathered.

A dark-red Molas Formation paleosol developed on a karst-modified, chemically weathered paleosurface on top of the Leadville Limestone. The Pennsylvanian Molas Formation consists of calcareous shale, mudstone, sandstone, and conglomerate averaging about 50 m thick. The overlying Pennsylvanian Hermosa Formation, as much as 550 m thick, consists of a stratigraphically complex, alternating sequence of near-shore silty shale to arkosic sandstone with interbedded marine limestone characteristic of transgressive-regressive cyclic deposition. The Hermosa and overlying Permian Cutler Formations are the most volumetrically extensive Paleozoic units in the Animas River watershed study area.

The Cutler Formation consists of feldspar-rich sandstone, red shale, mudstone, conglomerate, and rare, thin limestone beds. To the west of the Animas River downstream of Silverton, Permian Cutler Formation red beds as much as 300 m thick terminate the Paleozoic section. Cutler Formation rocks in the South Fork Mineral Creek subbasin have locally been contact metamorphosed to hornfels by Tertiary stocks clustered near peak 3,792 m (fig. 4; Ringrose, 1982).

Additional discussion of the Paleozoic history can be found in Burbank (1930), Atwood and Mather (1932), Kelley (1957), Varnes (1963), Burrell (1967), Baars and See (1968), and Baars and Ellingson (1984).

Mesozoic Rocks

Mesozoic-age rocks are best exposed near the Animas River watershed margins, outside the Tertiary calderas in the headwater subbasins of South Fork Mineral Creek (pl. 1; Luedke and Burbank, 2000), where they record continued continental deposition through the Jurassic Period. The generally west dipping Late Triassic-age reddish-brown sandstone, siltstone, shale, and limestone of the Dolores Formation overlie the Permian Cutler Formation. As with the upper Paleozoic rocks, the source for these terrestrial deposits is the San Luis–Uncompahgre uplifts. The light-colored, crossbedded, cliff-forming, eolian Entrada Sandstone overlies the Dolores Formation. The Wanakah Formation is a slope-forming unit that overlies the Entrada Sandstone and consists of calcareous mudstone, brown to green shale, greenish-gray sandstone with gypsum nodules and stringers, and minor limestone near its base. The Morrison Formation, which caps the Jurassic sequence, is generally a slope-forming unit that consists of a lower ledge-forming sandstone (Salt Wash Member) and an upper gray to green mudstone (Brushy Basin Member) deposited in a fluvial to lacustrine environment. Members of the Morrison Formation have been mined for their uranium content throughout areas within and bordering the Colorado Plateau (Galloway and Hobday, 1983). In the headwater basins that flow to South Fork Mineral Creek, a 120-m thick sequence of Mesozoic-age rocks of the Entrada, Wanakah, and Morrison Formations is exposed in tributaries that drain into South Fork Mineral Creek.

The Cretaceous section becomes more important from a water-rock interaction standpoint farther south of the study area near Durango, Colo., where a more complete Cretaceous section attains a thickness of nearly 2,300 m (Baars and Ellingson, 1984). Near Durango, the Dakota Sandstone is composed of medium- to coarse-grained conglomeratic sandstone and shale that unconformably overlie the Jurassic Morrison Formation. Overlying and conformable with the Dakota Sandstone are the dark-gray to black, organic-rich, fossiliferous shales of the marine Mancos Shale. Along the Piedra River, located southeast and outside the study area, the cliff-forming Mesaverde Formation sandstones intertongue with and overlie the Mancos Shale. The Mesaverde Formation consists of buff to gray sandstone ledges separated by interbedded gray shale (Kottlowski, 1957). The organic-rich Lewis Shale intertongues with and overlies the Mesaverde Formation sandstones south of Durango. Fluvial sandstones and shales represented by the multicolored Pictured Cliffs Sandstone, Fruitland Formation, and Kirtland Shale cap the Cretaceous sequence and were deposited near the regressing Cretaceous seaway (Baars and Ellingson, 1984).

Cretaceous rocks in the study area consist of the Dakota Sandstone and overlying Mancos Shale. These rocks crop out in the headwaters of South Fork Mineral Creek and have a combined maximum thickness of about 300 m. Late Cretaceous magmatism in the western San Juan Mountains produced granodiorite dikes, sills, laccoliths, and small intrusive plugs that were emplaced west and north of the study area and accompanied a period of tectonism related to the Laramide orogeny (Varnes, 1963).

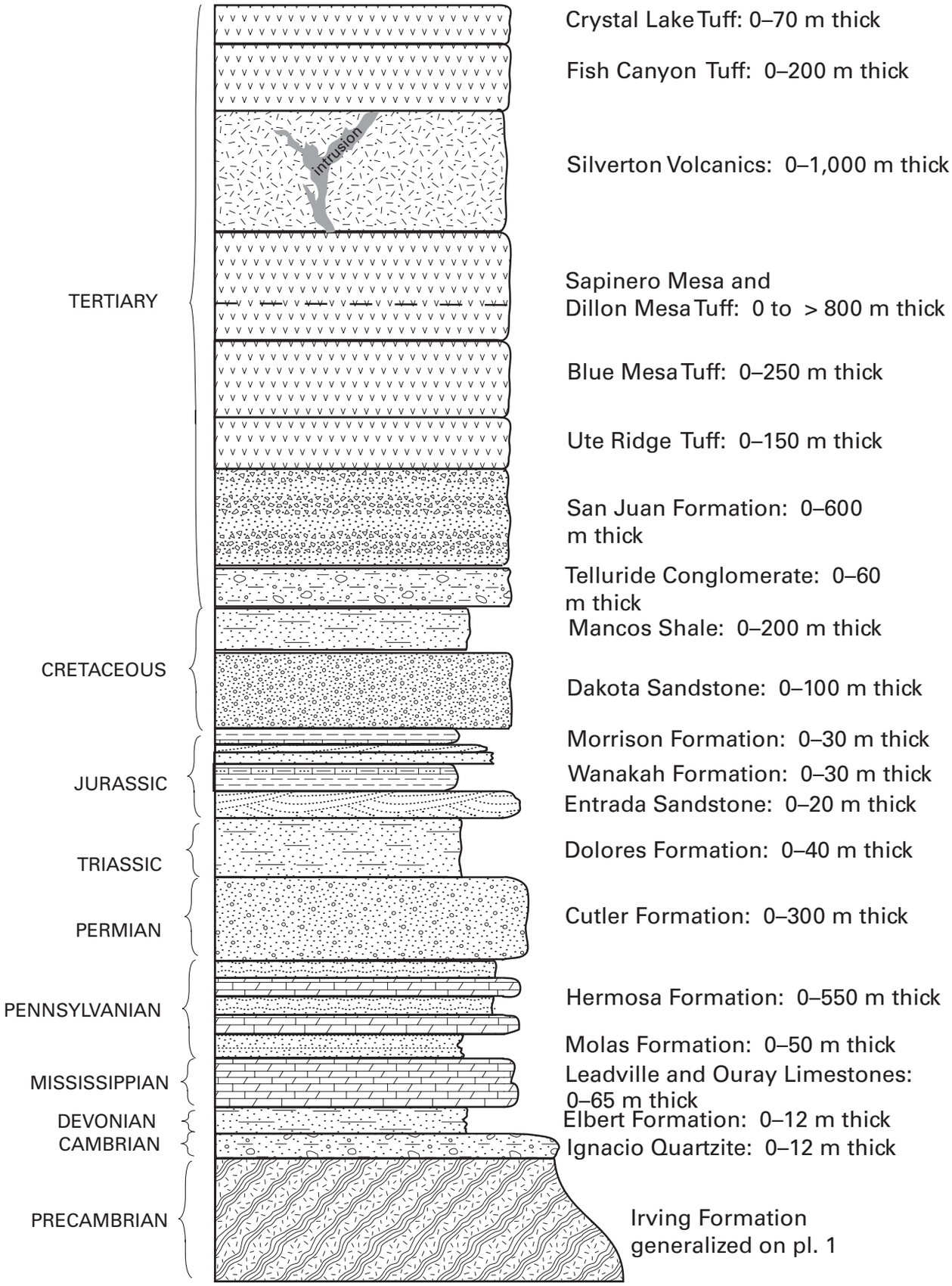
Crystal Lake Tuff: 0–70 m thick
Fish Canyon Tuff: 0–200 m thick
intrusion
Silverton Volcanics: 0–1,000 m thick
TERTIARY
Sapinero Mesa and
Dillon Mesa Tuff: 0 to > 800 m thick
Blue Mesa Tuff: 0–250 m thick
Ute Ridge Tuff: 0–150 m thick
San Juan Formation: 0–600
m thick
Telluride Conglomerate: 0–60
m thick
Mancos Shale: 0–200 m thick
CRETACEOUS
Dakota Sandstone: 0–100 m thick
Morrison Formation: 0–30 m thick
Wanakah Formation: 0–30 m thick
JURASSIC
Entrada Sandstone: 0–20 m thick
Dolores Formation: 0–40 m thick
TRIASSIC
Cutler Formation: 0–300 m thick
PERMIAN
Hermosa Formation: 0–550 m thick
PENNSYLVANIAN
Molas Formation: 0–50 m thick
Leadville and Ouray Limestones:
0–65 m thick
MISSISSIPPIAN
Elbert Formation: 0–12 m thick
DEVONIAN
CAMBRIAN
Ignacio Quartzite: 0–12 m thick
PRECAMBRIAN
Irving Formation
generalized on pl. 1

EXPLANATION

Crystal Lake Tuff (Oligocene)—Rhyolitic ash-flow tuff erupted from the Silverton caldera

Fish Canyon Tuff (Oligocene)—Dacitic ash-flow tuff erupted from the La Garita caldera east of study area

Silverton Volcanics (Oligocene)—Lava flows of intermediate composition and related volcaniclastic sedimentary rocks in addition to minor silicic lavas and ashflows

Sapinero Mesa Tuff (Oligocene)—Rhyolitic ash-flow tuff erupted from the San Juan and Uncompahgre calderas

Dillon Mesa Tuff (Oligocene)—Rhyolitic ash-flow tuff probably derived from the Uncompahgre caldera

Blue Mesa Tuff (Oligocene)—Rhyolitic ash-flow tuff probably derived from the Lost Lake caldera

Ute Ridge Tuff (Oligocene)—Dacitic ash-flow tuff derived from the Ute Creek caldera

San Juan Formation (lower Oligocene)— Intermediate-composition lava flows and volcaniclastic deposits consisting mostly of mudflow breccias

Telluride Conglomerate (Eocene)—Conglomerate and sandstone. Consists of Precambrian, Paleozoic, and Mesozoic clasts in a silty to sandy matrix

Mancos Shale (Upper Cretaceous)—Marine shale

Dakota Sandstone (Upper Cretaceous)—Sandstone with interbedded siltstone and carbonaceous shale

Morrison Formation (Upper Jurassic)—Sandstone with lenses of mudstone. Upper part is primarily calcareous mudstone

Wanakah Formation (Upper Jurassic)—Calcareous mudstone and siltstone with thin limestone and sandstone interbeds near top

Entrada Sandstone (Middle Jurassic)—Crossbedded sandstone

Dolores Formation (Upper Triassic)—Siltstone and sandstone with interbeds of limestone and conglomerate

Cutler Formation (Lower Permian)—Shale, arkosic sandstone, and conglomerate, locally calcareous

Hermosa Formation (Upper and Middle Pennsylvanian)—Interbedded silty shale to arkosic sandstone with interbedded marine limestone

Molas Formation (Middle and Lower Pennsylvanian)—Calcareous shale, sandstone, and conglomerate

Leadville and Ouray Limestones (Lower Mississippian and Upper Devonian)—Altered, mineralized, and recrystallized in and near study area

Elbert Formation (Upper Devonian)—Dolomitic limestone and interbedded calcareous shale and sandstone

Ignacio Quartzite (Upper Cambrian)—Quartzite, sandstone, and siltstone; locally conglomeratic

Irving Formation (Precambrian)—Interlayered banded amphibolite, gneiss, and minor sericite-biotite-chlorite schists

Figure 3 (above and facing page). Stratigraphic column for rocks in Animas River watershed study area. See also plate 1 for more detailed description of map units.

Tertiary Sedimentary Rocks

The Tertiary section begins with the Eocene Telluride Conglomerate, which was deposited on an extensive Eocene erosion surface (Mayor and Fisher, 1972). Lower layers within the Telluride Conglomerate contain rounded to subangular cobbles of Mesozoic and Paleozoic red sandstone and limestone. The upper layers contain mostly rounded to subangular clasts of Precambrian gneiss, schist, and quartzite, with minor quantities of granitic, volcanic, and sedimentary rocks in an arkosic, iron-oxide-stained, calcite-cemented matrix. The depositional sequence reflects an inverted paleostratigraphy owing to progressively deeper levels of erosion of Mesozoic through Precambrian basement rocks (Baars and Ellingson, 1984). To the west of the study area near Mount Wilson, the unit is more than 300 m thick; to the northeast, the unit thins to a maximum thickness of approximately 65 m, and it is absent in some areas over the San Juan dome. Within the Animas River watershed study area and vicinity, the Telluride Conglomerate overlies Paleozoic and Mesozoic sedimentary rocks in the South Fork Mineral Creek basin, and it overlies Paleozoic Hermosa and Cutler Formations above and west of the Animas River south of Silverton.

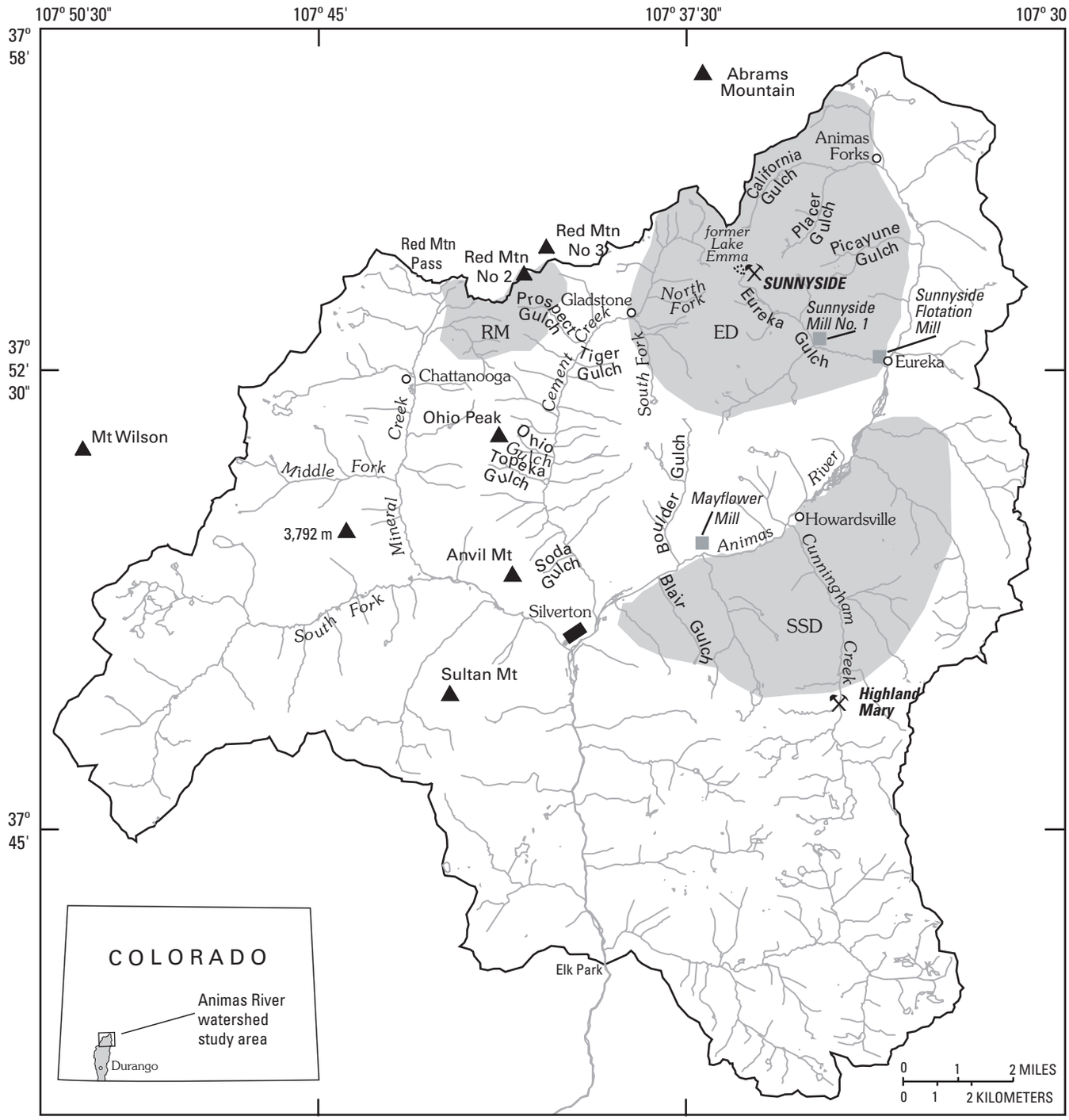

Figure 4. Geographic features, and mining districts referred to in this chapter. Shaded areas are generalized boundaries of three of the major mining districts. RM, Red Mountain mining district; ED, Eureka mining district; SSD, South Silverton mining district. Crossed pick and shovel, inactive mine discussed in report.

The upper Telluride Conglomerate includes intermediate-composition volcanics and volcaniclastic rocks and records the onset of early, mid-Tertiary volcanism. Hydrothermal polymetallic replacement ores containing copper-lead-gold-silver-zinc formed in the Telluride Conglomerate along northwest-trending caldera-related veins, dikes, and structures. These deposits were extensively mined beginning in 1948 (Mayor and Fisher, 1972; Jones, this volume, Chapter C).

Mid-Tertiary Volcanic Rocks

The Tertiary volcanic rocks in the San Juan Mountains blanketed more than 25,000 km^2, forming one of the great epicontinental volcanic piles of intermediate- to silicic-composition volcanic rocks. In general, onset of mid-Tertiary volcanism records construction of stratovolcanoes and volcanic shields built up by thick accumulations of andesite to rhyolite flows and breccias that were followed by several eruption cycles of more silicic ash flows. The eruption of ash flows led to caldera formation and local subsidence.

Precaldera Rocks

Mid-Tertiary volcanism in the San Juan Mountains commenced between 35 and 30 Ma with the eruption and deposition of voluminous calc-alkaline, intermediate-composition (52–63 percent SiO_2) lava flows, flow breccias, volcaniclastics, minor mafic tuffs, and abundant mudflows of the San Juan Formation (Lipman and others, 1973; Steven and Lipman, 1976). The San Juan Formation lavas are typically porphyritic and consist of plagioclase, clinopyroxene, hornblende, and opaque oxide primary phases. Within the study area, volcanic rocks are typically propylitically altered, and replacement of amphibole, pyroxenes, and plagioclase by secondary chlorite, epidote, calcite and locally sericite is pervasive.

Different geologists working in different parts of the western San Juan Mountains have assigned several formation names to time-equivalent San Juan Formation units. In the western San Juan region, intermediate-composition rocks of the Lake Fork Formation (Larsen and Cross, 1956) and the Picayune Formation (Burbank and Luedke, 1969) are all temporally equivalent to the San Juan Formation (Lipman and others, 1973; Lipman, 1976b). San Juan Formation is the name used herein. Collectively, the San Juan Formation units along with the other early intermediate-composition lava flows of the San Juan volcanic field make up the largest volume of eruptive products in the San Juan Mountains (Lipman, 1984). The 35 to 30 Ma San Juan and Picayune lavas are predominantly andesites and basaltic andesites; one single analysis plots in the trachyandesite field (fig. 5).

San Juan Formation volcanic rocks in the study area crop out near the northern, western, and southern topographic margin of the San Juan caldera (pl. 1) and attain a thickness of several hundred meters. Southwest of Silverton, in subbasins above South Fork Mineral Creek, the San Juan Formation unconformably overlies the Telluride Conglomerate and the Cutler Formation. Farther to the south, the San Juan Formation unconformably rests on Paleozoic strata and Precambrian rocks.

San Juan–Uncompahgre Caldera and Silverton Caldera Rocks

From 30 to 23 Ma, numerous eruptions formed multiple calderas (fig. 6), and related volcanic units were deposited throughout the San Juan volcanic field (Lanphere, 1988; Lipman and others, 1997; Bove and others, 2001). Two caldera events took place in the study area: the 28.2 Ma San Juan–Uncompahgre caldera complex and the younger, nested 27.6 Ma Silverton caldera (fig. 6; pl. 1) (Bove and others, 2001). The San Juan caldera in the study area is the southwest half of the roughly dumbbell shaped San Juan–Uncompahgre caldera complex (fig. 6). Prior to caldera formation, magma chambers were likely emplaced at shallow (from 9 to 5 km) depths in the crust (Johnson and Rutherford, 1989; Lipman and others, 1997) and differentiated to erupt relatively silicic (68 and 72 percent SiO_2) pyroclastic flows. Tertiary calderas in the western San Juans produced more than 1,000 km^3 of explosive volcanic products. For comparison, the volume of magma ejected from the San Juan–Uncompahgre caldera complex was >1,000 km^3, whereas the smaller, nested Silverton caldera ejected between 50 and 100 km^3 of magma (Lipman, 2000).

San Juan caldera eruptives include the intracaldera Eureka Member of the Sapinero Mesa Tuff and outflow Sapinero Mesa Tuff. The Sapinero Mesa Tuff is rhyolitic to dacitic in composition (fig. 5), containing phenocrysts of plagioclase, with lesser amounts of sanidine, biotite, and trace augite. The outflow sheet thickness averages 50 m; maximum thickness is 100 m. Outflow Sapinero Mesa Tuff is preserved on scattered high peaks to the west and northwest of the study area. In contrast, the San Juan caldera fill contains at least a 700-m section of densely welded and highly propylitized, intracaldera Eureka Member (Lipman and others, 1973). The Eureka Member is compositionally variable, has a lower silica content, and generally has a higher crystal content than the outflow equivalent Sapinero Mesa Tuff (fig. 5).

The Uncompahgre caldera, located northeast of the study area, formed in response to eruption of the Dillon Mesa Tuff; eruption of this tuff may have slightly preceded that of the San Juan caldera-related tuffs (Lipman and others, 1973). The Dillon Mesa Tuff, preserved mainly west of the study area, is relatively thin and is a crystal-poor rhyolite that is mineralogically similar to the rhyolitic phase of the outflow Sapinero Mesa Tuff.

Resurgent doming of the San Juan–Uncompahgre caldera complex began prior to infilling of the area by intermediate-composition lava flows (Lipman, and others, 1973). However,

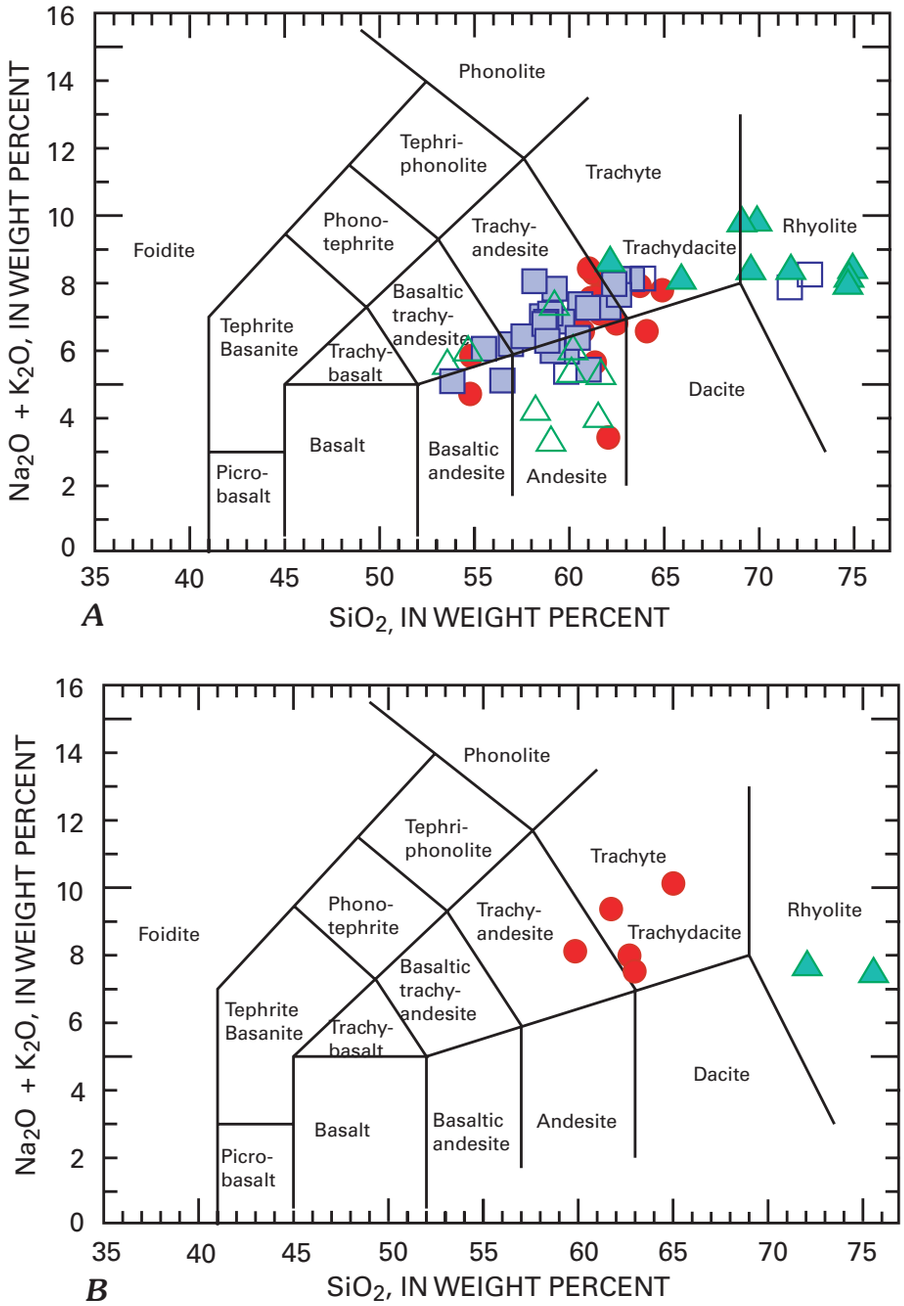

Figure 5. Total alkali versus silica classification (Le Bas and others, 1986). *A*, Intermediate-composition lava flows; solid circle, Silverton Volcanics, Burns Member; solid square, Silverton Volcanics, pyroxene andesite member; solid triangle, Eureka Member of the Sapinero Mesa Tuff; open square, undifferentiated lava flows; open triangle, San Juan Formation lava flow. *B*, Primarily silicic intrusives (GIS and Access database, Sole and others, this volume, Chapter G).

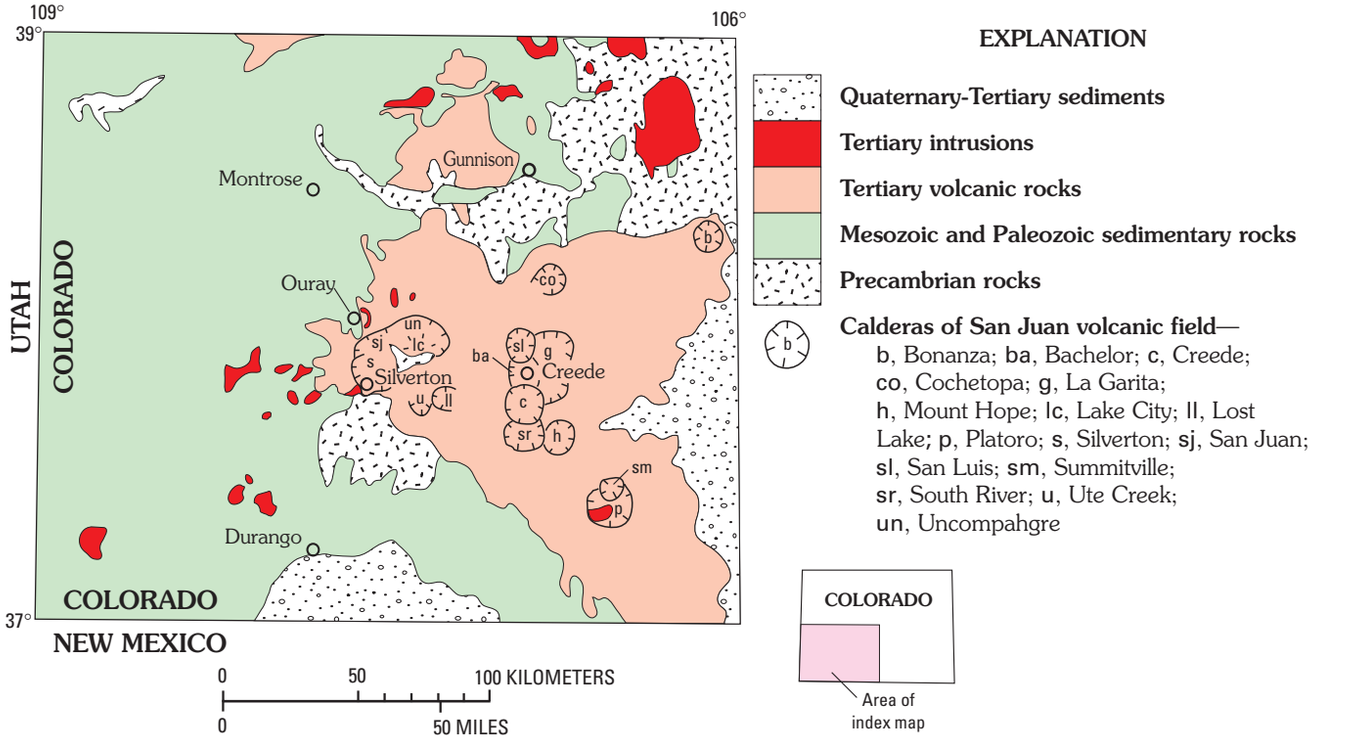

Figure 6. Regional map showing calderas of San Juan volcanic field and generalized rock types. Modified from Casadevall and Ohmoto (1977).

extensional fracturing during formation of the Eureka graben may have accommodated continued late-stage uplift of the San Juan–Uncompahgre resurgent dome. Eureka Member outcrops are exposed in the Eureka graben and southeast of Silverton along the margins of the caldera on the flanks of Kendall Mountain (pl. 1).

San Juan caldera activity culminated with ring fracture volcanism, the products of which constitute the Silverton Volcanics. These rocks fill the caldera depression to a thickness exceeding 1 km. Lavas are porphyritic and typically contain phenocrysts of plagioclase, amphibole, pyroxene, opaque oxides, and minor biotite in a fine-grained to aphanitic groundmass. Minor rhyolite to dacite ash-flow tuff consisting of quartz, biotite, potassium feldspar, plagioclase, and amphibole is preserved within the upper part of the Silverton Volcanics such as on Abrams Mountain, north of the Animas River watershed (Luedke and Burbank, 1961).

Most Silverton Volcanics lavas are subalkaline (fig. 7) as indicated by 58 samples examined during this study. With the exception of four samples, which plot as medium potassium andesites, the Silverton Volcanics lavas have high potassium concentrations (fig. 8). The intermediate- to silicic-composition Silverton Volcanics are divided into three interfingering members. The Burns Member is generally characterized by propylitically altered lavas and dacite to rhyolite tuffs. The pyroxene andesite member, which generally overlies the Burns Member, tends to be somewhat less altered. The volcaniclastic sedimentary rocks of the Henson Member interfinger with both the Burns and the pyroxene andesite members (Lipman, 1976b). The Burns Member has a trend toward higher silica compositions when compared with the commonly overlying, younger pyroxene andesite and Henson Member lavas. This relatively higher silica concentration trend in Burns Member lavas is shown in the strontium versus silica variation diagram (fig. 9).

Deposition of the Silverton Volcanics was closely followed by eruption of the Crystal Lake Tuff at 27.6 Ma, which resulted in formation of the Silverton caldera. The Crystal Lake Tuff is a crystal-poor, low-silica rhyolite (72 percent SiO_2) that contains phenocrysts of sanidine and plagioclase, biotite, and minor augite (Lipman and others, 1973). Outflow Crystal Lake Tuff is preserved outside of the Silverton caldera; accumulations of 25 to 50 km^3 have been recognized in regions toward the northeast, in the moat of the Uncompahgre caldera, and to the east-southeast in the upper Rio Grande drainage basin (Lipman and others, 1973). Intracaldera Crystal Lake Tuff has not been recognized within the Silverton caldera, and outflow remnants in the immediate vicinity outside the caldera are also quite small. The problem remains whether this unit was entirely removed within the Silverton caldera during subsequent erosion or if the magma chamber was largely evacuated and most if not all of the Crystal Lake Tuff was deposited as outflow. More detailed mapping of the Silverton caldera is needed to resolve this issue.

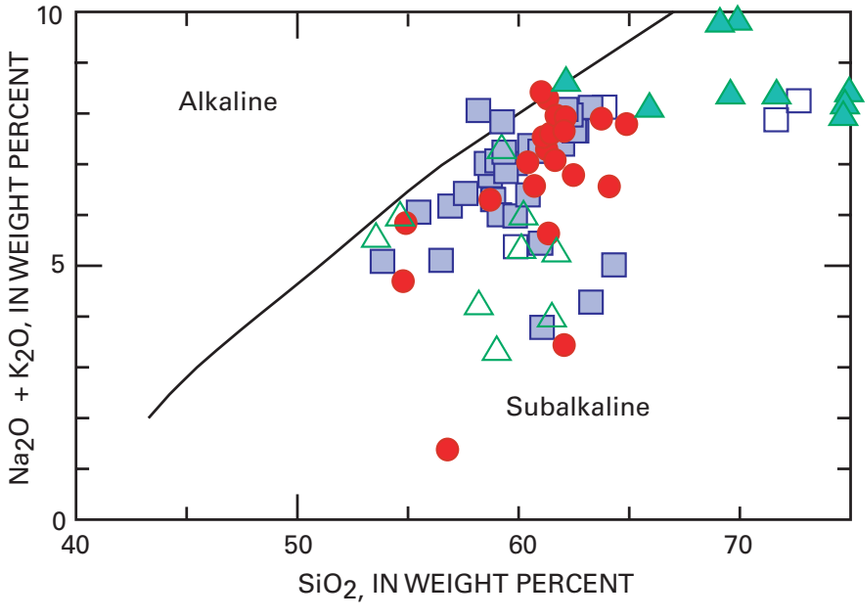

Figure 7. Total alkali versus silica, alkaline-subalkaline classification (Irvine and Baragar, 1971). Solid circle, Silverton Volcanics, Burns Member lava flows; solid square, Silverton Volcanics, pyroxene andesite member lava flows; open square, undifferentiated lava flows; solid triangle, Eureka Member of the Sapinero Mesa Tuff; open triangle, San Juan Formation lava flows (GIS and Access database, Sole and others, this volume, Chapter G).

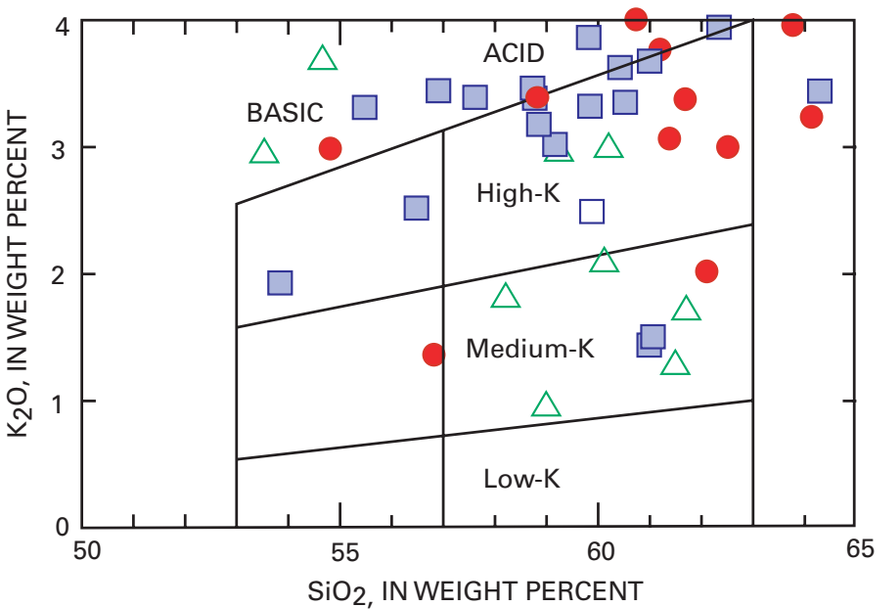

Figure 8. Potassium versus silica classification (Gill, 1981). Solid circle, Silverton Volcanics, Burns Member lava flows; solid square, Silverton Volcanics, pyroxene andesite member lava flows; open square, undifferentiated lava flows; open triangle, San Juan Formation lava flows (GIS and Access database, Sole and others, this volume, Chapter G). K, potassium.

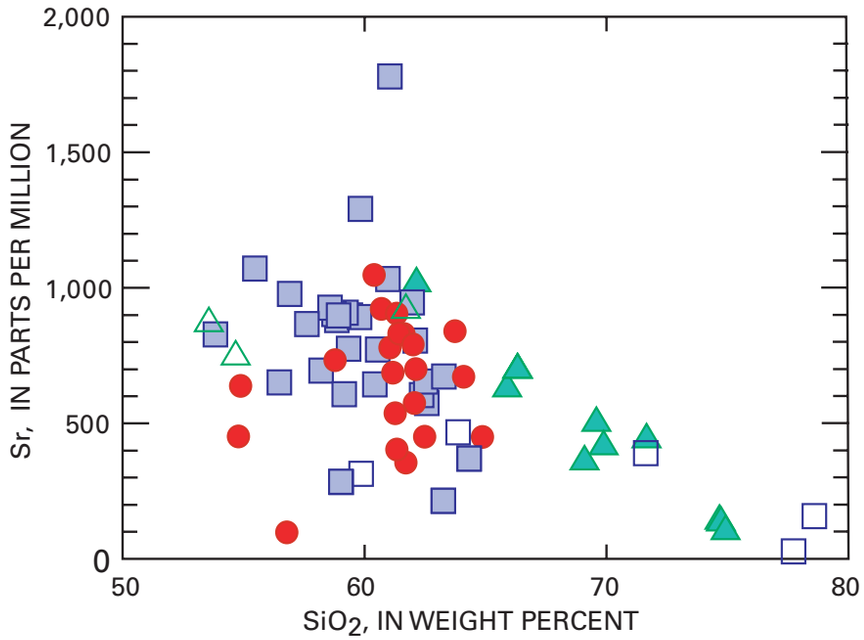

Figure 9. Strontium (parts per million) versus silica classification. Solid circle, Silverton Volcanics, Burns Member lava flows; solid square, Silverton Volcanics, pyroxene andesite member lava flows; open square, undifferentiated lava flows; solid triangle, Eureka Member of the Sapinero Mesa Tuff; open triangle, San Juan Formation lava flows (GIS and Access database, Sole and others, this volume).

Beginning approximately 1 million years after Silverton caldera formation, numerous stocks, dikes, and other silicic intrusions formed along the Silverton caldera ring fracture zone. The oldest postcaldera granitic stocks (monzonite, monzodiorite, granodiorite, and monzogranite) are about 26.6 Ma and intruded along the southern part of the Silverton caldera ring fracture (Lipman and others, 1976; Ringrose, 1982; Bove and others, 2001). These porphyry stocks contain plagioclase, potassium feldspar, quartz, biotite, clinopyroxene, and opaque oxides. This late-stage igneous activity was accompanied by hydrothermal alteration and formation of a contemporaneous low-grade, molybdenum-copper porphyry deposit and cogenetic polymetallic vein deposits (Ringrose, 1982; Musgrave and Thompson, 1991). Concentric and radial caldera-related structures were paths of least resistance for the later mineralizing fluids (Varnes, 1963; Casadevall and Ohmoto, 1977; Bove and others, this volume, Chapter E3). Most granitic intrusives are altered to varying degrees, and mafic minerals such as biotite and pyroxene are replaced by chlorite. Late-stage, 23 to 10 Ma dacitic to rhyolitic intrusions emplaced along the north and northwest structural margin of the Silverton caldera were concomitant with hydrothermal alteration and related mineralization (Bove and others, this volume). Dacitic intrusions dated at 23 Ma in the Red Mountain mining district are coarsely porphyritic, containing large (1 cm) phenocrysts of potassium feldspar, plagioclase, quartz, and biotite in a fine-grained groundmass. Younger, circa 10 Ma rhyolite intrusions are generally finely crystalline, porphyritic to aphanitic, and consist primarily of quartz and potassium feldspar. These granitic intrusions and younger late-stage dacitic to rhyolitic composition intrusions of the Red Mountain mining district are mostly calc-alkalic (fig. 10).

Intrusions in the Red Mountain district and elsewhere appear to be geographically correlated with a high fracture density (Bove and others, this volume), and they have brecciated margins that are possibly more permeable than nonbrecciated surrounding country rocks where not filled with quartz and other gangue minerals. Therefore, the brecciated intrusive margins may strongly influence ground-water flow where a higher fracture density coincides with possible permeability contrasts between intruded country rocks and brecciated margins.

Mineralized breccia pipes are closely associated with some of the silicic intrusions in the Red Mountain mining district (Fisher and Leedy, 1973; Nash, 1975). The geology and geochemistry of the breccia pipe ores are important because the ores have high sulfur concentrations and contain silver-bearing copper and lead sulfosalts of arsenic and antimony and base-metal sulfides (Fisher and Leedy, 1973; Bove and others, this volume). These deposits and associated mine waste weather to produce some of the highest arsenic concentrations in stream sediments in the watershed study area (Bove and others, this volume; Church, Fey, and Unruh, this volume, Chapter E12).

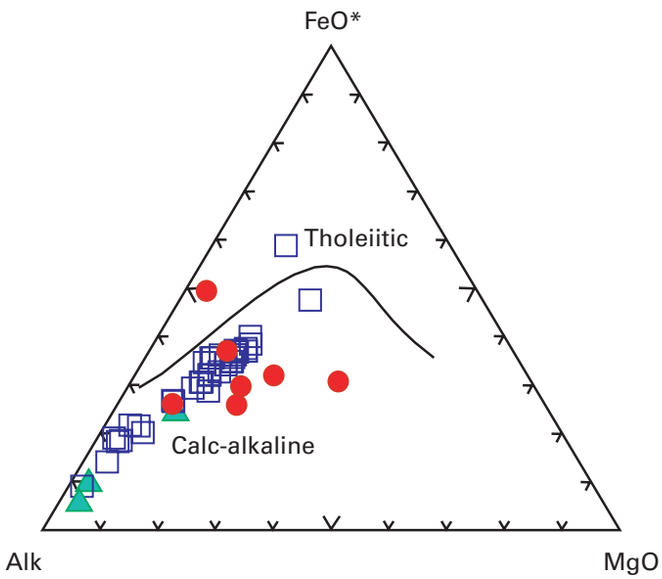

Figure 10. Total alkali, total iron and magnesium, tholeiitic versus calc-alkaline classification. Solid circle, dacite porphyries; open square, granitic to diabase intrusions; triangle, rhyolite intrusion (GIS and Access database, Sole and others, this volume).

Tertiary Structures and Veins of the San Juan–Uncompahgre and Silverton Calderas

Structures that developed coincident with volcanic activity were utilized as flow paths by later mineralizing solutions, and the resulting mineralized areas were economically mined for base-metal sulfides and precious metals (Varnes, 1963; Casadevall and Ohmoto, 1977; Bove and others, this volume). The structures related to the San Juan–Uncompahgre and Silverton calderas are pervasive features that reflect the complex volcanotectonic history of the study area.

Five dominant structural elements are related to formation of the San Juan–Uncompahgre and Silverton calderas: (1) circular and likely overlapping caldera ring fault zones, (2) a topographic margin associated with the San Juan caldera that marks the topographic expression generally found outward from the structural margin, (3) a northeast-trending graben (Eureka graben) formed during resurgent doming of the central core of the San Juan–Uncompahgre caldera, (4) radial faults and vein structures located principally near the northwest and southeast periphery of the San Juan and Silverton calderas, and (5) thousands of mineralized and barren veins and vein structures, many of which lack surface expressions. These structural elements related to the San Juan–Uncompahgre and Silverton calderas are discussed as follows.

Caldera Ring Faults

The 28.2 Ma San Juan and nearly contemporaneous Uncompahgre calderas form a dumbbell-shaped (fig. 6) double caldera complex separated by a segment of Precambrian basement. The caldera complex has an elongate dimension of 48×24 km and formed along a northeast-southwest trend parallel to the Colorado mineral belt. It has been proposed that the northeast-southwest alignment of the long axis of the San Juan and Uncompahgre volcanic depression coincides with Precambrian basement structures of the Colorado mineral belt, which were perhaps reactivated during the episode of Tertiary-age volcanism (Tweto and Sims, 1963; Burbank and Luedke, 1969). A ring fault system developed simultaneously with collapse of the San Juan–Uncompahgre caldera system. The San Juan caldera ring fault is observed in underground workings of the Highland Mary, Green Mountain, and Pride of the West mines (Church, Mast, and others, this volume, Chapter E5) where Precambrian Irving Formation rocks are in vertical contact with Eureka Member of the Sapinero Mesa Tuff along the south margin of the caldera (Luedke and Burbank, 2000). When the San Juan–Uncompahgre caldera collapsed along the approximately 24 km diameter piston-shaped ring fault zone, the Sapinero Mesa Tuff was erupted and deposited outside the caldera as outflow. Simultaneous with caldera collapse, the Eureka Member of the Sapinero Mesa Tuff ponded within the interior of the San Juan caldera to a thickness of 700 m with no base exposed (Lipman and others, 1973).

The 27.6 Ma Silverton caldera is nested within the older San Juan caldera. The Silverton caldera is one of the least studied calderas in the region. Its collapse is evidenced by (1) the intensely faulted and fractured ring fracture zone, well exposed along the Mineral Creek basin (fig. 11) and east of Silverton along the Animas River (pronounced erosion along Mineral Creek and along the Animas River upstream from Silverton accentuates the semicircular drainage system that follows the Silverton caldera ring fault zone (fig. 12)), and (2) several hundred meters of downfaulting of both the Eureka Member and the Silverton Volcanics along the Silverton caldera ring fracture (Burbank, 1933; Varnes, 1963; Lipman and others, 1973) (fig. 13).

San Juan Caldera Topographic Margin

The geomorphic expression of the San Juan caldera is indicated by a highland topographic margin that defines the arcuate headwater regions of the Animas River in upper Maggie Gulch, Cunningham Creek, and along Deer Park Creek south of Kendall Mountain (pl. 1). Small to large, meso- to megabreccia blocks of older basement rocks and Eureka Member have caved inward from the steep topographic walls. North-dipping Paleozoic limestone units south of Silverton and megabreccia limestone blocks at the headwaters of Cunningham Creek (pl. 1) near the Highland Mary mine delineate the southern

Figure 11. Highly fractured and weakly mineralized intermediate-composition Silverton Volcanics lavas along Silverton caldera structural margin, near confluence of Mineral Creek and Middle Fork Mineral Creek.

topographic margin of the San Juan caldera. Rocks along the margin of the San Juan–Uncompahgre caldera have caved into the caldera during and after eruption, forming an inward-sloping surface of the topographic margin. The San Juan caldera topographic margin in the study area is located near the headwater regions of the South Silverton mining district where Precambrian, Paleozoic, and older Tertiary rocks are in contact with the Eureka Member of the Sapinero Mesa Tuff. Meso- to megabreccia blocks that have caved into the caldera also are present near the eastern San Juan caldera topographic margin near the mouth of Picayune Gulch along the upper Animas River above Eureka.

Eureka Graben Faults and Formation of Radial Fracture Pattern

Collapse of the San Juan–Uncompahgre caldera complex was followed closely by resurgence. Contemporaneous with resurgence, an elliptical dome 15 km wide by 30 km long formed between the two calderas, and extensional fracturing over the resurgent dome resulted in Eureka graben formation. The Sunnyside and Toltec faults define the northeastern part of the Eureka graben; the Ross Basin and Bonita faults that formed in the southwestern part of the graben border the west-northwest-trending part of the graben (pl. 1). Each of the Eureka graben faults has lateral and vertical extents of thousands of meters. Eureka graben structures were later extensively mineralized with base and precious metals. Late Silverton caldera resurgence has been postulated, to have been facilitated by reactivation of Eureka graben faults and by regional concentric and radial fractures (Smith and Bailey, 1968). However, Lipman and others (1973) suggested that it is difficult to distinguish any Silverton caldera resurgence from the broad resurgent doming that occurred over the earlier and much larger calderas.

An intricate system of radial fractures developed that are especially abundant in the northwest and southeast sides of the San Juan caldera. This radiating fracture system likely formed during resurgent doming, and thus the area affected by resurgence extended beyond the San Juan caldera margin (Lipman and others, 1973). Many of the structures of the Eureka graben and radiating fracture system were later mineralized and became economic exploration targets for base-metal sulfides and precious metals. Nonetheless, the continued reactivation of the Eureka graben after San Juan caldera resurgence is one cause of the extensive mineralization of these structures. Some of the most metal-rich veins fill the Eureka graben faults. These are the Ross Basin, Sunnyside, Bonita, and Toltec vein systems (pl. 1).

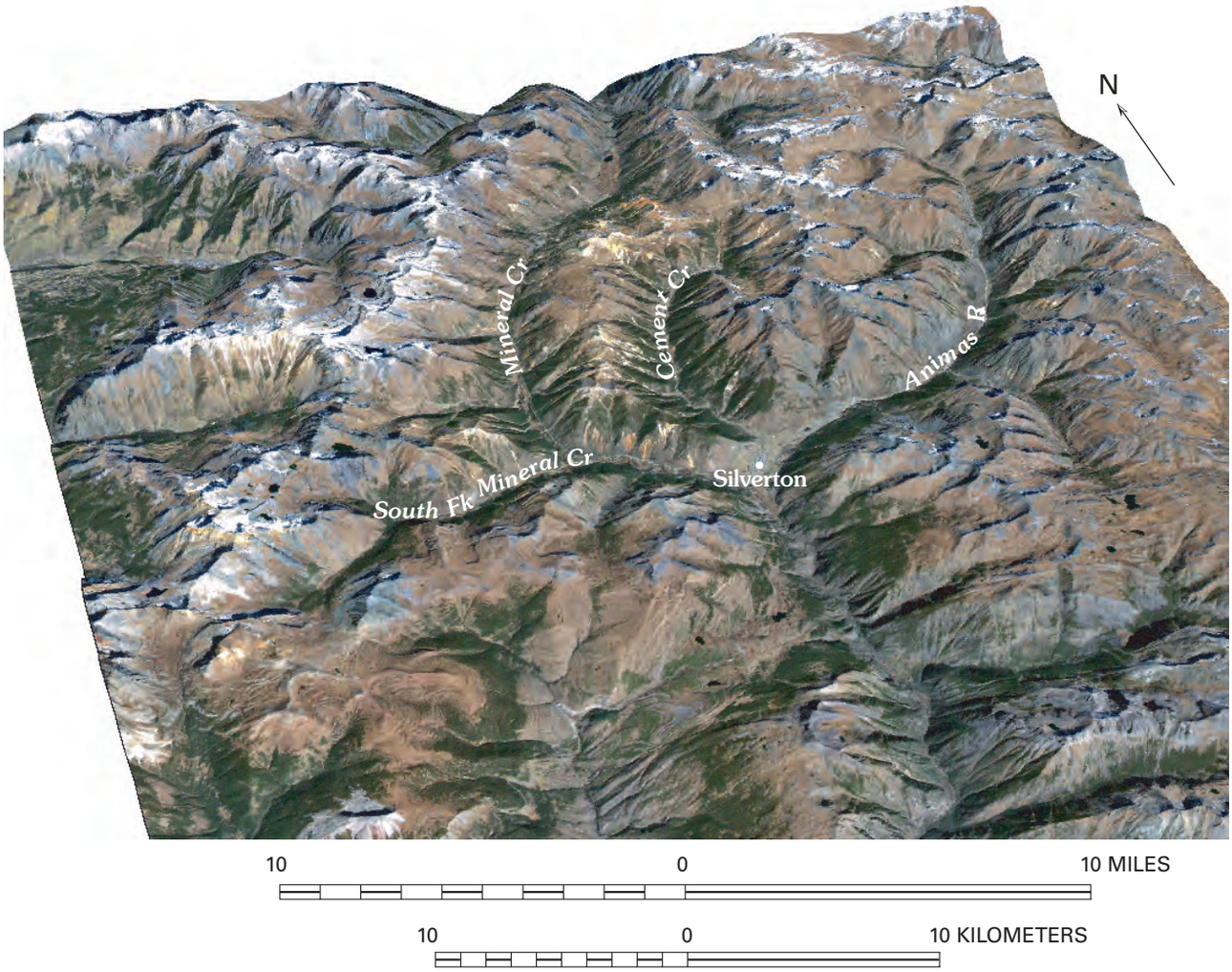

Figure 12. Erosion along structural margin of Silverton caldera by Mineral Creek and Animas River has resulted in an arcuate, semicircular drainage pattern that accentuates area occupied by the Silverton caldera. Nonvegetated areas north of South Fork Mineral Creek and between Mineral and Cement Creeks are areas of hydrothermal alteration. (Remote sensing processing by R.R. McDougal.)

Mineralized Faults and Fractures

Thousands of veins occur at and (or) below the surface in the vicinity of the nested San Juan and Silverton calderas. Vein orientation in the mining districts near Silverton appears to have a strong control on whether veins are highly mineralized. In the South Silverton area, located southeast of Silverton, veins that are parallel to the caldera ring faults are only weakly mineralized (Varnes, 1963). It is the radial, northwest-oriented veins that are the most highly mineralized features. Veins in the study area, such as those of the Shenandoah-Dives deposits, have lateral extents exceeding 3 km and were mined through a vertical extent of greater than 300 m. Similarly, it is the northwest-trending veins near the northwest periphery of the Silverton caldera near the Camp Bird mine that are also highly mineralized (Hutchinson, 1988). In contrast, structures related to the Eureka graben had a strong influence in controlling ore deposition in the Sunnyside mine (Casadevall and Ohmoto, 1977). Sunnyside mine vein systems are focused near the intersection of the Sunnyside and Bonita faults. The Sunnyside mine workings beneath Eureka Gulch exposed mineralized vein structures that are parallel to the Eureka graben (fig. 2; pl. 1), which contain strongly developed northeast- to northwest-trending mineralized veins. The workings of the Sunnyside vein deposits were mined through a lateral and vertical extent of 2,100 m and 610 m respectively. Common vein minerals identified in vein systems of the Sunnyside mine workings are listed in table 1; vein minerals of the Sunnyside mine workings that occur with less than 0.5 percent abundance are listed in table 2 (Casadevall and Ohmoto, 1977).

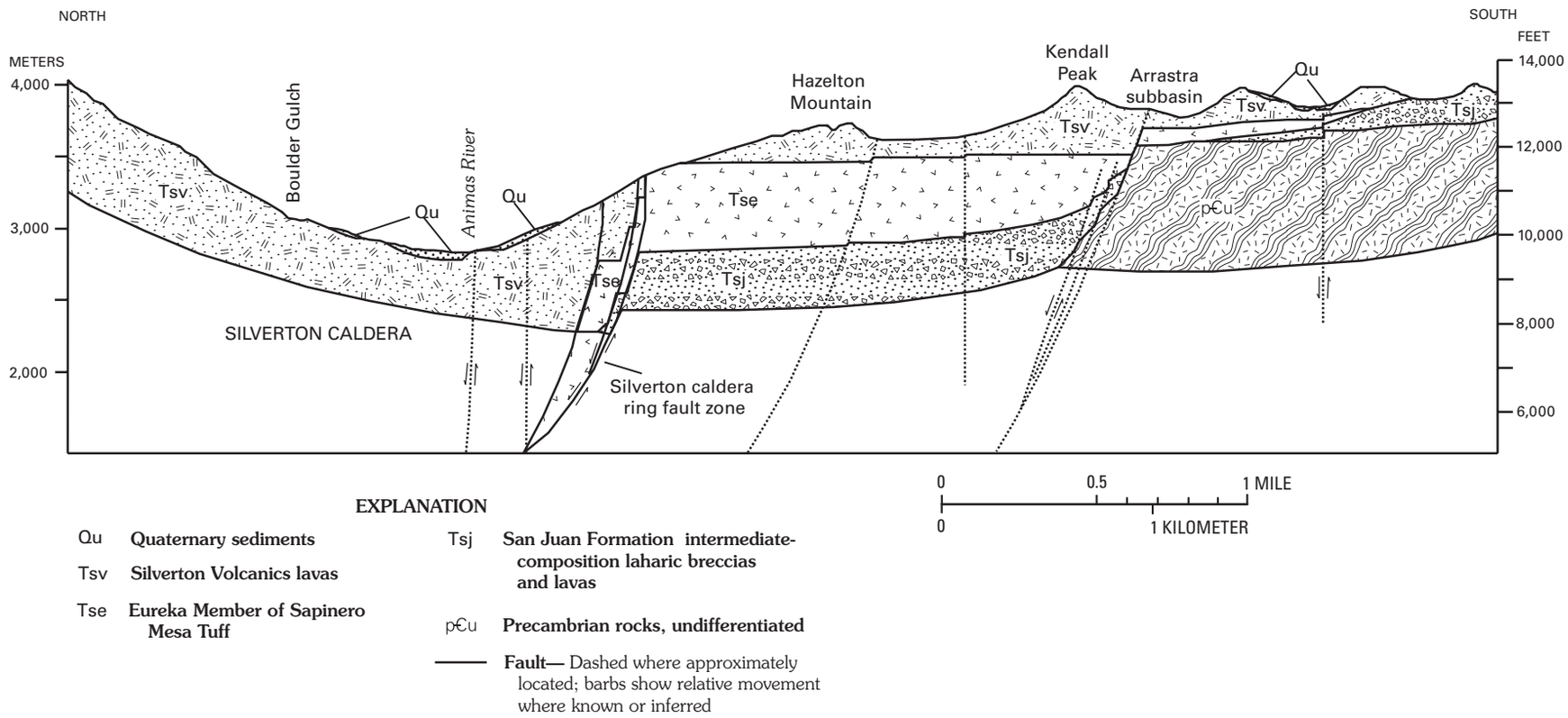

Figure 13. Generalized cross section (modified from Luedke and Burbank, 2000), showing structural offset along ring fault zone of Silverton caldera. Note Eureka Member of the Sapinero Mesa Tuff exposed above valley floor to the south of Animas River; no Eureka Member is exposed in vicinity of Boulder Gulch.

Table 1. Major vein minerals of the Sunnyside mine workings.

[Minerals listed in decreasing volume percent abundance]

	Vol. pct
quartz (SiO_2)	30–35
sphalerite (ZnS)	10–15
galena (PbS)	10–15
pyroxmangite ($MnSiO_3$)	10–15
pyrite (FeS_2)	6–8
rhodochrosite ($MnCO_3$)	5–8
chalcopyrite ($CuFeS_2$)	3–5
tetrahedrite ($Cu_{12}Sb_4S_{13}$)	1–4
fluorite (CaF_2)	1
calcite ($CaCO_3$)	1

Table 2. Minor (<0.5 volume percent) vein minerals of the Sunnyside mine workings.

hematite (Fe_2O_3)	gold (Au)
petzite ($AuAg_3Te_2$)	calaverite ($AuTe_2$)
alabandite (MnS)	huebnerite ($MnWO_4$)
tephroite (Mn_2–SiO_4)	friedelite ($Mn_8Si_6O_{18}$)
helvite ($Mn_4(Be_3Si_3O_{12})S$)	anhydrite ($CaSO_4$)
sericite (KAl_2 $(AlSi_3O_{10})(OH_2)$	aikinite ($PbCuBiS_3$)
bornite (Cu_5FeS_4)	barite ($BaSO_4$)
gypsum ($CaSO_4(2H_2O)$)	

Implications of Caldera Faults and Veins as Flow Paths

Caldera ring faults and associated veins of the Eureka graben and radial vein structures near the margin of the nested San Juan and Silverton calderas (pl. 1) are laterally and vertically continuous. Thus, these features may be important ground-water flow paths. Veins in the study area have widths that range from less than 1 m to 30 m. The wider veins are best described as vein zones that consist of an anastomosing network of multiple veins. Not all vein systems, however, are open fluid flow paths for ground water today. Several veins that were mined as part of the Sunnyside mine workings, which are exposed at the surface in Eureka and Placer Gulches, are annealed with quartz and reveal little open space for fluid migration. However, a vein that is filled at the surface can be heterogeneous: it can display open cavities at depth that could provide flow paths for ground water if such cavities were interconnected and continuous. Multiple fractures also crosscut veins in many places, which allows for penetration of water and thus exposes minerals within vein interiors to weathering.

The inward-sloping surface of the arcuate San Juan caldera topographic margin is an angular unconformity that should also be considered as a potential ground-water flow path. This is especially true in the region near the South Silverton mining district, where the topographic surface likely dips toward the north in the subsurface toward the center of the Silverton caldera. The chaotic and fragmental nature of deposits along the topographic margin in the subsurface could provide a permeable flow path for ground water, where the related deposits are not completely sealed with gangue minerals, such as quartz, or with ore minerals.

In order to test the degree to which bedrock fractures and caldera-related structures influence water quality, conductivity geophysical surveys were used to map structures that contain conductive metal-rich water. The electromagnetic geophysical survey shows a conductive arcuate feature that coincides with the Silverton caldera ring fracture (Smith and others, this volume, Chapter E4). The importance of veins, lineaments, and structures as pathways for conductive, metal-rich waters, along with the correlation with geophysical signatures, is discussed further in later chapters (McDougal and others, this volume, Chapter E13; Smith and others, this volume).

Alteration Types

The effects of a long-lived cycle of volcanotectonic activity and multiple mineralization events that span more than 20 million years have resulted in five major alteration types in the study area (Bove and others, this volume). The multiple alteration and coincident mineralization events postdate caldera collapse, taking place between 26 and 10 Ma (Bove and others, 2001). For a detailed discussion of the alteration types, see Bove and others (this volume).

Airborne Visible and Infrared Imaging Spectrometer (AVIRIS) data (Dalton and others, this volume, Chapter E2) and detailed field map data were combined to produce regional and detailed alteration maps (Bove and others, this volume; Dalton and others, this volume). X-ray diffractometry was completed on whole-rock hand samples to independently verify alteration assemblages identified via AVIRIS and field mapping. These techniques are useful, especially when applied together to decipher alteration assemblages across broad regions, such as at the watershed scale.

The five major alteration types identified in the region are listed in increasing order of weakest to most intense, as follows: (1) propylitic, (2) weak sericite-pyrite, (3) vein-related quartz-sericite-pyrite, (4) quartz-sericite-pyrite, and (5) acid-sulfate (fig. 14). Those assemblages with a high acid-generating capacity include the weak sericite-pyrite, quartz-sericite-pyrite, vein-related quartz-sericite-pyrite, and acid-sulfate assemblages. A summary of the alteration types follows.

Regional Propylitic Alteration

Regional propylitic alteration identified by Burbank (1960) as a “pre-ore propylitization” event has affected most rocks in the vicinity of the San Juan–Uncompahgre and Silverton caldera complex. The mineralogy of this assemblage,

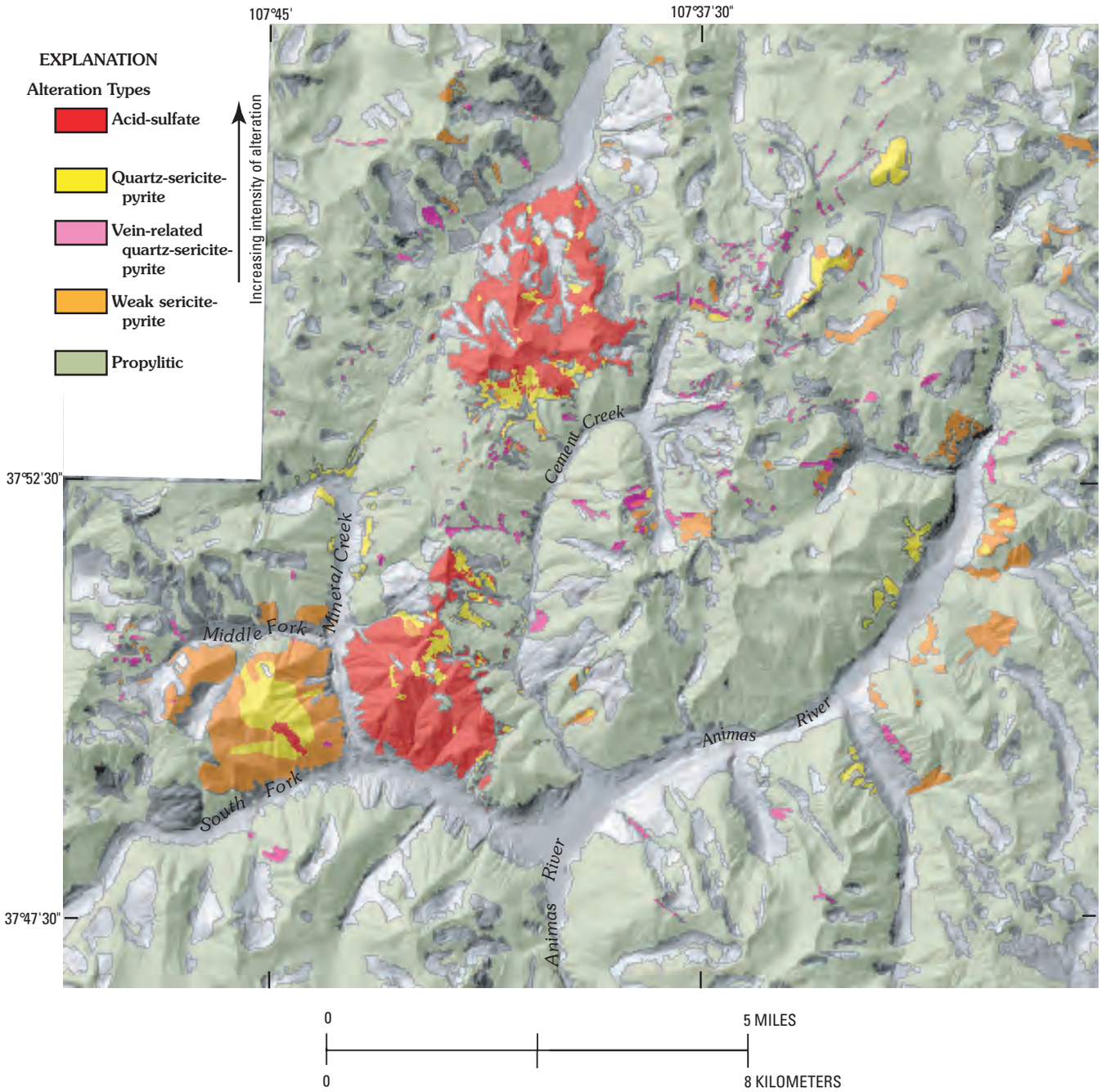

Figure 14. Generalized alteration map of Animas River watershed study area (Bove and others, this volume). Hillshaded, 10-m resolution digital elevation model used as base image.

although variable, consists of quartz, chlorite, epidote, calcite, albite, pyrite, and opaque oxides in the presence of unaltered to slightly altered primary feldspar crystals (fig. 15). This alteration type is thought to have formed during the period 28.2 Ma to about 27.6 Ma, as the nearly 1 km sequence of Silverton Volcanics lavas that infilled the San Juan caldera cooled, degassed, and literally stewed in their own volatiles. In the process of degassing, large quantities of CO_2, perhaps the primary rock-altering volatile component (among others such as H_2O and SO_2), were released, altering the original minerals and matrix of the country rock (Burbank, 1960). Rocks that have experienced this type of alteration commonly have a green tinge in outcrop owing to the presence of chlorite and epidote. The subsequent, more intense alteration and mineralization events in several places overprint the regionally pervasive propylitic alteration assemblage.

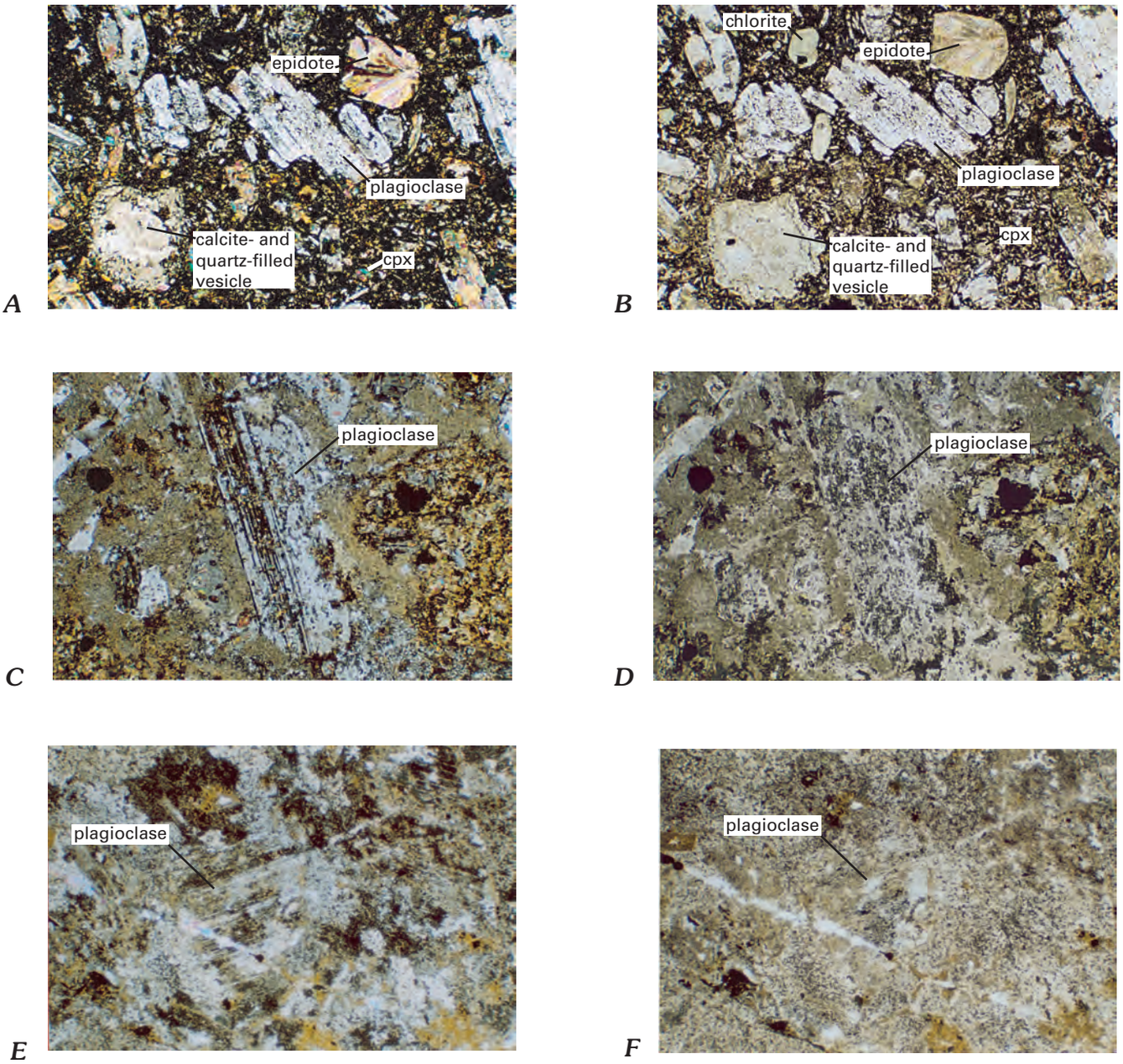

Figure 15. Photomicrograph pairs (crossed polars on left, plane light on right) of intermediate-composition volcanic rocks sampled from the study area. Each frame is about 3×4 mm. Letters *A–B*, Weakly propylitized andesite porphyry of the San Juan Formation collected near headwaters of Middle Fork Mineral Creek. Rocks are relatively fresh (note mottled but intact plagioclase); however, vesicles and groundmass are filled with chlorite, epidote, and calcite. *C–D*, Propylitized intermediate-composition lava flows from the Silverton Volcanics, sampled near Sunnyside mine. Rock is porphyritic and composed of plagioclase, quartz, clinopyroxene, and opaque oxides. Greenish-gray hue of groundmass is typical of propylitic assemblage and is caused by microcrystalline chlorite and epidote. *E–F*, More strongly propylitized Silverton Volcanics sampled about 300 m from *C*, *D*. Note more highly altered plagioclase (faint polysynthetic twinning) and felty matrix consisting of chlorite and epidote. Most if not all study area rocks have been affected by some degree of propylitic alteration; higher grades of alteration locally obliterate all primary mineral phases.

Weak Sericite-Pyrite Alteration

The weak sericite-pyrite assemblage is found in areas of densely spaced veins and adjacent to areas of the more intensely altered quartz-sericite-pyrite assemblage. Quartz, sericite (synonymous with illite for fine muscovite), and pyrite characterize this assemblage, as do weakly altered to unaltered plagioclase and chlorite. One of the largest areas of weak sericite-pyrite altered rock is present near the periphery of a low-grade copper-molybdenum porphyry system centered near peak 3,792 m between South Fork Mineral Creek and Middle Fork Mineral Creek (fig. 4) (Ringrose, 1982; Yager and others, 2000). The more weakly altered rocks affected by this alteration appear similar to the propylitic assemblage in outcrop, but they can be distinguished by the abundance of pyrite along dense fractures and somewhat lesser presence of magnetite, epidote, and chlorite along fractures.

Vein-Related Quartz-Sericite-Pyrite Alteration

Vein-related zones of quartz-sericite-pyrite alteration have formed adjacent to mineralized single veins or vein zones, such as those adjacent to and within the Eureka graben. A northeast-southwest-trending 2.4 km wide by 6.6 km long area of relatively densely spaced vein-related quartz-sericite-pyrite altered rock occurs between Houghton Mountain on the northeast and Minnesota Gulch to the southwest. This vein swath is generally centered near and may be related to fractures that formed in the resurgent core of the San Juan caldera. Other areas of vein-related quartz-sericite-pyrite alteration have formed along radial fractures outside the San Juan caldera margin.

Quartz-Sericite-Pyrite Alteration

Generally, all the primary minerals that constituted the original host rock are altered in the quartz-sericite-pyrite assemblage throughout relatively large areas. Primary feldspars and mafic minerals are altered to a fine-grained rock of quartz, sericite, and pyrite. In outcrop, rocks are bleached white; fresh pyrite is observed on freshly broken, unweathered surfaces. Sericite resembles very fine muscovite with a sugary texture. Where this assemblage has been oxidized, jarosite and goethite coat weathered surfaces and stain the outcrops light yellowish green to various shades of brown. Only weathered pyrite casts along with sericite and quartz remain in oxidized outcrops. Some areas that are highly affected by quartz-sericite-pyrite alteration include that of peak 3,792 m (fig. 4), the region near Ohio Peak, Houghton and California Mountains, and upper Prospect Gulch.

Acid-Sulfate Alteration

This alteration assemblage is characterized by the mineral assemblages of quartz-alunite and quartz-pyrophyllite, with some argillic alteration zones. Alunite in some outcrops near Red Mountain is fine grained, pinkish white, and relatively soft; it has replaced quartz and rectangular phenocrysts as much as 1 cm across. All primary minerals have been obliterated and replaced by the mineral assemblages mentioned. There are two regions of acid-sulfate alteration. One broad area of acid-sulfate alteration is centered near Red Mountain Nos. 1–3; another formed along Anvil Mountain between the headwaters of Ohio Gulch and a location about 0.6 km to the southeast of Zuni Gulch north of Silverton. Outcrops are commonly bleached white or stained brown by adjacent oxidized mineralized veins.

Acid-Generating Capacity of Non-Mining-Affected Rocks

One excellent example of the strong influence that alteration has on water quality is observed near the low-grade molybdenum-copper porphyry deposit near peak 3,792 m (fig. 4). The acid-generating capacity of non-mining-affected rocks related to the weak sericite-pyrite and quartz-sericite-pyrite assemblages is clearly documented in the east- to northeast-flowing tributary that enters Middle Fork Mineral Creek to the north of peak 3,792 m (fig. 4). The headwaters of this tributary originate in San Juan Formation rocks and have a pH that ranges from 6.5 to 6.8. In contrast, farther downstream, the acid-generating capacity of these rocks increases dramatically as surface water interacts with the weak sericite-pyrite and quartz-sericite-pyrite altered San Juan Formation rocks and porphyry intrusive rocks: pH drops below 3.5 (Mast and others, 2000; Mast and others, this volume, Chapter E7; Wright, Simon, and others, this volume, Chapter E10). This is one excellent example among many others in the study area where alteration has a strong influence on water quality (Bove and others, this volume; Mast and others, this volume; Wright, Simon, and others, this volume).

Acid-Neutralizing Capacity of Study Area Rocks

Hydrothermal alteration and mineralization have obliterated phases that aid in mitigating acid rock drainage in several regions of the study area. However, sedimentary rocks that contain calcite, and volcanic and other igneous rocks that have been altered to the propylitic assemblage chlorite-epidote-calcite, have a moderate to high acid-neutralizing capacity.

Metamorphic Rock Acid-Neutralizing Capacity

The Precambrian Irving Formation, consisting of amphibolite, gneiss, and schist, is important for its potentially high acid-neutralizing capacity. Regional uplift, tilting to the west, and subsequent retrograde metamorphism of Irving Formation

rocks (Steven and others, 1969) resulted in formation and concentration of the acid-neutralizing mineral assemblage of chlorite-epidote-calcite (Desborough and Driscoll, 1998; Desborough and Yager, 2000). The Precambrian Irving Formation, although not compiled separately from other Precambrian units in this study, is exposed in the southern part of the area of plate 1. Areas where surface water interacts with Precambrian Irving Formation rocks include the headwaters of Cunningham Creek, the Animas River downstream of Silverton at the mouth of Deadwood Gulch, and other tributaries downstream including the area drained by Deer Park Creek.

Sedimentary Rock Acid-Neutralizing Capacity

Both the Ouray and Leadville Limestone units are important for their high acid-neutralizing capacity in the upper Animas River canyon where sediment weathered from these rocks reaches the Animas River. The Hermosa and overlying Permian Cutler Formations are the most volumetrically extensive Paleozoic units in the upper part of the watershed. These units are important because they are in some areas calcite bearing (Burrell, 1967). They therefore have a high acid-neutralizing capacity that is realized where weathering and erosion contribute reworked Cutler and Hermosa sediment to South Fork Mineral Creek and to the Animas River downstream of Silverton. The Telluride Conglomerate commonly contains abundant limestone clasts and locally may provide a high acid-neutralizing capacity. However, this unit is volumetrically minor in comparison with other calcareous sedimentary units; on a regional scale it likely does not have a large acid-neutralizing effect in the study area.

Tertiary Volcanic Rock Acid-Neutralizing Capacity

Quantitative investigations by Desborough and Yager (2000) on rocks of the watershed study area attest to the relatively high acid-neutralizing capacity of igneous bedrock. Most if not all of the volcanic rocks in this area were subjected to a regional propylitic alteration event that replaced the primary magmatic mineral phases amphibole, pyroxene, and plagioclase with secondary chlorite, epidote, and calcite. Sericite is locally pervasive. Calcite fills vesicles and microfractures (figs. 15, 16), floods the groundmass in lava flows and in volcaniclastic rocks (Bove and others, this volume), and thereby contributes to the high acid-neutralizing capacity of these rocks (Desborough and Yager, 2000).

Regionally, the large volume of San Juan Formation volcanic rocks available for water-rock interaction has a strong influence on water quality, depending on the amount of secondary propylitic minerals and textural characteristics.

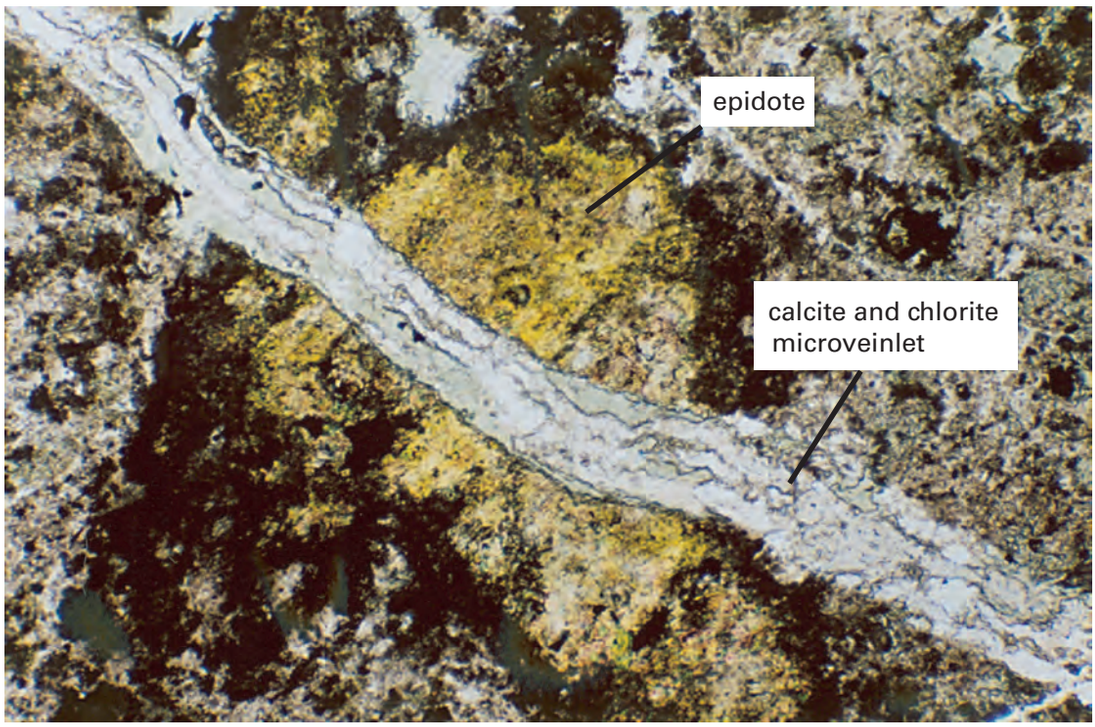

Figure 16. Photomicrograph of propylitized intermediate-composition Silverton Volcanics lava flow, with calcite and chlorite microveinlet. Full frame is about 1 mm by 2 mm.

The enhanced water-rock interaction of this formation results from its large volume of porous and permeable volcaniclastic rocks, with only relatively minor and highly fractured lava flows.

The Silverton Volcanics, in the core of the San Juan and Silverton calderas, is very important both volumetrically and for its high acid-neutralizing capacity. Where not intensely altered, most of the Silverton Volcanics have experienced propylitic alteration. Propylitization of the Silverton Volcanics is thought to have occurred as volatiles such as CO_2, SO_2, and H_2O degassed from the cooling, 1-km thick volcanic pile (Burbank, 1960). Silverton Volcanics lavas that lack calcite but contained abundant chlorite were still found to have a 10 weight percent (calcite equivalent) acid-neutralizing capacity (Desborough and Yager, 2000). Locally, the Silverton Volcanics have the strongest influence on water quality, depending on the amount of secondary propylitic minerals that impart a high acid-neutralizing capacity (Desborough and Yager, 2000), the degree of hydrothermal alteration, and textural characteristics. Lava flow foliation in the vicinity of Boulder Gulch and along Mineral Creek follows the dip of the central resurgent dome toward the west and south. The flow foliation facilitates fluid transport and promotes water-rock interaction. Surface water that passes through propylitically altered volcanics in Boulder Gulch has near-neutral pH (Mast and others, this volume, Chapter E7). However, Silverton Volcanics host the majority of mineral deposits mined in the Silverton region (Bejnar, 1957; Casadevall and Ohmoto, 1977), and in areas where late-stage hydrothermal alteration introduced acid-generating minerals, such as pyrite in Prospect Gulch, acid-neutralizing capacity is eliminated and acidic drainage can have a pH as low as 2.6 (Bove and others, this volume; Mast and others, this volume).

Postcaldera intrusions of the Sultan Mountain and peak 3,792 m granitic stocks also underwent propylitic alteration, altering the primary mafic minerals such as biotite to chlorite. Acid-neutralization experiments performed on these propylitically altered intrusives indicate an acid-neutralizing capacity as high as that of the Silverton Volcanics lavas that lack calcite (Desborough and Yager, 2000).

Surficial Deposit Acid-Neutralizing Capacity

Weathering of acid-sulfate mineralized bedrock and subsequent deposition of weathered material in downslope surficial deposits will result in acid generation, as ground water infiltrates and reacts with pyrite and other acid-generating minerals. In contrast, surface water infiltrating surficial deposits containing abundant propylitic rocks with the mineral assemblage chlorite-epidote-calcite will probably undergo some reduction in acidity (Desborough and Yager, 2000; Yager and others, 2000; Wirt and others, this volume, Chapter E17).

Late Tertiary Erosion

Neogene erosion denuded much of the San Juan Mountains volcanic cover. In places canyon cutting has amounted to as much as 1,520 m (Smith and Bailey, 1968). This period of erosion has long been referred to as the “canyon cycle of erosion” (Lee, 1917). The high potential for erosion developed during this time owing to differential displacement of the San Juan Mountains relative to the incipient, adjacent Rio Grande Rift basin to the east and post-mid-Tertiary extensional tectonic terrain. Chapin and Cather (1994) estimated Precambrian bedrock offset in adjacent mountain ranges and basins to gauge the amount of late Tertiary relative displacement. Using this technique they determined that an average of 5 km of relative displacement of Precambrian rocks has occurred. They further estimated from basin stratigraphy that from 7 to 30 times more sediment was supplied to the Rio Grande Rift basin during the Miocene to Pliocene than in the Pleistocene. Clearly, late Tertiary erosion was important in exposing large surface areas of mineralized bedrock and metalliferous veins to weathering, in the Animas River watershed study area. Steven and others (1995) suggested that regional uplift and tilting from 5 to 2 Ma, concurrent with continued active rifting in the Rio Grande Rift to the east, further accelerated erosion and canyon cutting throughout the uplifted area.

Molinar and England (1990) proposed an alternative hypothesis for the increased erosion rates. They suggested that increased erosion rates during the late Cenozoic may be due to climate change. A trend toward lower temperatures and stormier climate could greatly contribute to increased erosion in the San Juan Mountains and subsequent deposition of alluvial fans adjacent to mountain ranges.

Glaciation Events

Pleistocene, Wisconsin-age glaciation greatly altered the San Juan landscape (Atwood and Mather, 1932; Gillam, 1998). The San Juan ice sheet was one of the largest (second only to the Yellowstone-Absaroka) to form south of the upper-mid-latitude Laurentide ice sheet (Atwood and Mather, 1932; Leonard and others, 1993). The San Juan ice sheet covered approximately 5,000 km^2, was as much as 1,000 m thick, covered all but the highest peaks, and formed piedmont glaciers that extended to the adjacent foothill areas (Atwood and Mather, 1932).

Unstable slope conditions developed after glacier retreat. Weathering processes in glaciated cirque basins and mountain valleys have resulted in accumulation of large volumes of talus, debris cone, and landslide deposits. The mineral constituents present in the surficial deposits will influence the acid-generating or neutralizing capacity of these deposits.

Pleistocene to Holocene Fluvial Geomorphologic Conditions

The numerous surficial deposits in the watershed study area serve as porous and permeable pathways for surface-water infiltration and ground-water flow. From GIS analysis of the geology polygon coverage (Sole and others, this volume, Chapter G), Yager and Bove have estimated that 27 percent of the bedrock in the watershed is covered by between 1 and 5 m or more of Pleistocene to Holocene sedimentary deposits (pl. 1). These deposits formed as a result of mass wasting of weathered bedrock outcrops and accumulated in cirque basins and on slopes and in valleys to form talus, landslides, and colluvium. Alluvial processes have formed multiple generations of stream terraces (Gillam, 1998) and caused deposition of alluvial fans and flood-plain sediments along main drainages and their tributaries (Blair and others, 2002).

The surficial deposits are important in the context of abandoned mine land investigations because deposits that formed prior to mining record the geochemical baseline of sediments that were deposited by natural processes. These have been analyzed and compared with deposits that formed after the onset of mining to determine how the geochemical baseline has changed once mining commenced (Church and others, 1997; Vincent and others, 1999; Blair and others, 2002; Church, Fey, and Unruh, this volume).

Surficial deposits are also the principal precipitation sites for iron-rich water that is initially derived from oxidation of pyrite by acidic water and then precipitated to form ferricrete deposits. Ferricrete deposits are iron oxyhydroxide cemented clastics, or nonclastic bog iron (Verplanck and others, this volume, Chapter E15, and this report, pl. 2). Radiocarbon dates on logs preserved in ferricrete deposits range from modern to 9,000 yr B.P. (Verplanck and others, this volume). A relationship exists between upslope sources of acidic drainage, mineralized bedrock, structures, and the Holocene surficial deposits where ferricrete has formed that substantiates the inferred link between acidic water and ferricrete deposits (Vincent and others, this volume, Chapter E16; Wirt and others, this volume; this report, pl. 2).

Current studies indicate that geologic processes affecting erosion prior to mining have not changed dramatically in the past 15,000 years (Vincent and others, this volume). Around the end of the 19th century, however, mill wastes were dumped into streams and transported throughout the river system (Nash, 2000; Vincent and others, 1999; Nash and Fey, this volume). This affected the Animas River's hydrology. For example, mill waste that was reworked by floods below Eureka town between 1900 and 1930 resulted in sediment aggradation along a low-gradient reach of the upper Animas River (Blair and others, 2002). These fluvial tailings included some concentrated metal-rich stamp mill tailings, as well as extensive tailings deposits from the Sunnyside Eureka Mill (Jones, this volume; Church, Mast, and others, this volume). The effect of dumping mill tailings into the streams was a dramatic impact on vegetation health, and especially on bank-stabilizing willows that were characteristic of the upper Animas River riparian zone prior to mining (Vincent and others, 1999; Vincent and Elliott, this volume, Chapter E22).

Elsewhere, the fluvial geomorphology in basins such as Cement Creek appears to have been minimally affected by mining (Vincent and others, this volume). This is not to say, however, that mining has not altered historical water compositions. Tracer injection studies along Cement Creek have identified the principal trace- and major-element loading sources (Kimball and others, this volume, Chapter E9).

Although the overall geomorphology of the present Cement Creek basin has not been greatly modified, sudden storms can cause rapid movement of large volumes of mineral-bearing and acid-generating sediment. These events occur frequently and confound watershed characterization efforts. On August 26, 1997, one such storm upstream of Silverton sent thousands of cubic meters of sediment pouring into Cement Creek, principally from Topeka and Ohio Gulches. Furthermore, geochemical analyses of debris-flow sediments collected from the August 26 event indicated high concentrations of iron (6.8 weight percent) and aluminum (9.0 weight percent). Laboratory passive leach experiments indicated that these deposits also had a high potential to generate acidity. The following year, the 1998 spring stream runoff transported any sediment that remained along the banks of Topeka Gulch from the previous summer's storm event, into Cement Creek.

Summary

One goal of this abandoned mine lands study was to investigate the influence that the diverse volcanic lithology and alteration assemblages have on the geochemical baseline and on water quality in the Animas River watershed. A 1-km thick, weakly to intensely altered and mineralized, intermediate- to felsic-composition volcanic cover largely determines water-rock interaction and water quality in the core of the Animas River watershed study area. Subsequent regional, low-grade propylitic alteration resulted in formation and concentration of the acid-neutralizing mineral assemblage of chlorite-epidote-calcite. Replacement of primary mineral phases by the propylitic acid-neutralizing mineral phases is pervasive in the core and areas surrounding the Silverton and San Juan calderas. Later caldera structures associated with the Tertiary volcanics served as conduits for late-stage hydrothermal mineralizing fluids, which overprinted the earlier regional propylitic alteration event. Mineralization changed the primary mineral assemblage of host rocks and either eliminated or improved their acid-neutralizing capacity, depending on the intensity and type of alteration. Faults of multiple ages and orientations, bedding dip, and fracture density and orientation further dictate fluid flow and influence the surface- and ground-water drainage from the alpine basins to the adjacent valleys.

Miocene to Pliocene erosion and Pleistocene glaciation exposed the Animas River watershed study area to extensive weathering and erosion to form surficial deposits that constitute as much as 27 percent of surface area exposures. Where these surficial deposits are derived from sulfatarically altered and mineralized bedrock, they serve as porous and permeable pathways that permit ground water to react with acid-generating minerals to produce acid water and load soluble major and trace elements to streams. In contrast, where these surficial deposits are derived from bedrock of the propylitic assemblage, they permit ground water to react with acid-neutralizing minerals and hence have the potential to neutralize acid drainage.

The red, yellow, and white precipitates from water draining hydrothermally altered rock and many mine sites are a strong visual indication of the effects that geology and mining have had on water quality in some tributary basins near Silverton, Colo. The environment is that of an extensively fractured and altered, mountainous watershed and water-storage system, which can supply either acid-generating or acid-neutralizing water, depending on the composition of minerals in the transport media (for example, fractured bedrock aquifer, porous surficial deposit, mine-waste pile, and (or) fluvial environment) and the amount of surface-water and ground-water interaction that transpires along a flow path in any of these transport media.

References Cited

Atwood, W.W., and Mather, K.F., 1932, Physiography and Quaternary geology of the San Juan Mountains, Colorado: U.S. Geological Survey Professional Paper 166, 176 p.

Baars, D.L., and Ellingson, J.A., 1984, Geology of the western San Juan Mountains, *in* Brew, D.C., ed., Paleotectonics, San Juan Mountains, Dolores Formation, paleosols and depositional systems, Jurassic depositional systems, San Juan Basin, Quaternary deposits and soils, Durango area: Rocky Mountain Section, Geological Society of America 37th Annual Meeting, Fort Lewis College, Durango, Colo., p. 1–45.

Baars, D.L., and See, P.D., 1968, Pre-Pennsylvanian stratigraphy and paleotectonics of the San Juan Mountains, southwestern Colorado: Geological Society of American Bulletin, v. 79, p. 333–349.

Bailey, R.G., 1995, Description of the ecoregions of the United States: United States Department of Agriculture Miscellaneous Publication 1391, 108 p.

Barker, Fred, 1969, Precambrian geology of the Needle Mountains, southwestern Colorado: U.S. Geological Survey Professional Paper 644–A, p. A1–A35.

Bejnar, Waldemere, 1957, Lithologic control of ore deposits in the southwestern San Juan Mountains, *in* Kottlowski, F.E., and Baldwin, Brewster, eds., Guidebook of southwestern San Juan Mountains, Colorado: New Mexico Geological Society 8th Annual Field Conference Guidebook, p. 162–173.

Blair, R.W., Jr., Yager, D.B., and Church, S.E., 2002, Surficial geologic maps along the riparian zone of the Animas River and its headwater tributaries, Silverton to Durango, Colorado, with upper Animas River watershed gradient profiles: U.S. Geological Survey Digital Data Series 071.

Bove, D.J., Hon, Ken, Budding, K.E., Slack, J.F., Snee, L.W., and Yeoman, R.A., 2001, Geochronology and geology of late Oligocene through Miocene volcanism and mineralization in the Western San Juan Mountains, Colorado: U.S. Geological Survey Professional Paper 1642, 30 p.

Burbank, W.S., 1930, Revision of geologic structure and stratigraphy in the Ouray District of Colorado, and its bearing on ore deposition: Colorado Scientific Society Proceedings, v. 12, p. 151–232.

Burbank, W.S., 1933, Vein systems of the Arrastre basin and regional geologic structure in the Silverton and Telluride Quadrangles, Colorado: Colorado Scientific Society Proceedings, v. 13, 214 p.

Burbank, W.S., 1960, Pre-ore propylization, Silverton Caldera, Colorado, *in* Geological Survey research 1960: U.S. Geological Survey Professional Paper 400–B, article 6, p. B12–B13.

Burbank, W.S., and Luedke, R.G., 1968, Geology and ore deposits of the San Juan Mountains, Colorado, *in* Ridge, J.D., ed., Ore deposits of the United States, 1933–1967, the Graton-Sales Volume, Volume 1: New York, American Institute of Mining, Metallurgical, and Petroleum Engineers, p. 714–733.

Burbank, W.S., and Luedke, R.G., 1969, Geology and ore deposits of the Eureka and adjoining districts, San Juan Mountains, Colorado: U.S. Geological Survey Professional Paper 535, 73 p.

Burrell, S.D., 1967, Geology of an area southwest of Silverton, San Juan County, Colorado: Boulder, Colo., University of Colorado M.S. thesis, 106 p., 21 figs., 1 plate.

Casadevall, Thomas, and Ohmoto, Hiroshi, 1977, Sunnyside mine, Eureka mining district, San Juan County, Colorado—Geochemistry of gold and base metal ore deposition in a volcanic environment: Economic Geology, v. 92, p. 1285–1320.

Chapin, C.E., and Cather, S.M., 1981, Eocene tectonics and sedimentation in the Colorado Plateau–Rocky Mountain area: Arizona Geological Society Digest, v. 14, p. 173–198.

Chapin, C.E., and Cather, S.M., 1994, Tectonic setting of the axial basins of the northern and central Rio Grande rift: Geological Society of America Special Paper 291, p. 5–25.

Church, S.E., Kimball, B.A., Fey, D.L., Ferderer, D.A., Yager, T.J., and Vaughn, R.B., 1997, Source, transport, and partitioning of metals between water, colloids, and bed sediments of the Animas River, Colorado: U.S. Geological Survey Open-File Report 97–151, 135 p.

Cross, Whitman, Howe, Ernest, and Ransome, F.L., 1905, Description of the Silverton quadrangle, Colorado: U.S. Geological Survey Geological Atlas, Folio 120, 34 p., 4 maps.

Desborough, G.A., and Driscoll, Rhonda, 1998, Mineralogical characteristics and acid-neutralizing potential of drill core samples from eight sites considered from metal-mine related waste repositories in northern Jefferson, Powell, and Lewis and Clark counties, Montana: U.S. Geological Survey Open-File Report 98–0790, 6 p.

Desborough, G.A., and Yager, D.B., 2000, Acid-neutralizing potential of igneous bedrocks in the Animas River headwaters, San Juan County, Colorado: U.S. Geological Survey Open-File Report 00–0165, 14 p.

Epis, R.C., and Chapin, C.E., 1975, Geomorphic and tectonic implications of the post-Laramide, late Eocene erosion surface in the southern Rocky Mountains, *in* Curtis, B.F., ed., Cenozoic history of the southern Rocky Mountains: Geological Society of America Memoir 144, p. 45–74.

Fisher, F.S., and Leedy, W.P., 1973, Geochemical characteristics of mineralized breccia pipes in the Red Mountain district, San Juan Mountains, Colorado: U.S. Geological Survey Bulletin 1381, 43 p.

Galloway, W.E., and Hobday, D.K., 1983, Terrigenous clastic depositional systems, applications to petroleum, coal, and uranium exploration: New York, Springer-Verlag, Inc., 423 p.

Gill, J.B., 1981, Orogenic andesites and plate tectonics: Berlin, Springer, 389 p.

Gillam, M.E., 1998, Late Cenozoic geology and soils of the lower Animas River valley, Colorado and New Mexico: Boulder, Colo., University of Colorado Ph. D. dissertation, 477 p., 3 plates.

Hoch, A.R., Reddy, M.M., and Drever, J.I., 1999, Importance of mechanical disaggregation in chemical weathering in a cold alpine environment, San Juan Mountains, Colorado: Geological Society of America Bulletin, v. 111, p. 304–314.

Hutchinson, R.M., 1988, Structure and ore deposits of the Camp Bird Mine, Ouray, Colorado, *in* Hutchinson, R.M., ed., Epithermal base-metal and precious-metal systems, San Juan Mountains, Colorado: Society of Economic Geologists Guidebook Series, v. 3, p. 4–44.

Irvine, T.N., and Baragar, W.R.A., 1971, A guide to the chemical classification of the common volcanic rocks: Canadian Journal of Earth Science, v. 8, p. 523–548.

Johnson, M.C., and Rutherford, M.J., 1989, Experimentally determined conditions in the Fish Canyon Tuff, Colorado, magma chamber: Journal of Petrology, v. 30, p. 711–737.

Kelley, V.C., 1946, Geology, ore deposits, and mines of the Mineral Point, Poughkeepsie, and Upper Uncompahgre districts, Ouray, San Juan, and Hinsdale counties, Colorado: Proceedings of the Colorado Scientific Society, v. 14, p. 287–311.

Kelley, V.C., 1957, General geology and tectonics of the western San Juan Mountains, Colorado, *in* Kottlowski, F. E., and Baldwin, Brewster, eds., Guidebook of southwestern San Juan Mountains, Colorado: New Mexico Geological Society 8th Annual Field Conference Guidebook, p. 154–162.

Kluth, C.F., and Coney, P.J., 1981, Plate tectonics of the Ancestral Rocky Mountains: Geology, v. 9, p. 10–15.

Kottlowski, F.E., 1957, Mesozoic strata flanking the southwestern San Juan Mountains, Colorado and New Mexico, *in* Kottlowski, F. E., and Baldwin, Brewster, eds., Guidebook of southwestern San Juan Mountains, Colorado: New Mexico Geological Society 8th Annual Field Conference Guidebook, p. 138–153.

Lanphere, M.A., 1988, High resolution $^{40}Ar/^{39}Ar$ chronology of Oligocene volcanic rocks, San Juan Mountains, Colorado: Geochimica et Cosmochimica Acta, v. 52, p. 1425–1434.

Larsen, E.S., Jr., and Cross, Whitman, 1956, Geology and petrology of the San Juan Region, southwestern Colorado: U.S. Geological Survey Professional Paper 258, 303 p.

LeBas, M.J., LeMaitre, R.W., Streckeisen, A., and Zanettin, B., 1986, A chemical classification of volcanic rocks based on the total alkali silica diagram: Journal of Petrology, v. 27, p. 745–750.

Lee, W.T., 1917, The geologic story of Rocky Mountain National Park, Colorado: U.S. Department of the Interior, National Park Service, 89 p.

Leonard, Eric, Merritts, Dorothy, and Carson, Robert, 1993, Quaternary geology, upper Rio Grande drainage, San Juan Mountains, Colorado, *in* Wilson, M.A., compiler, The Sixth Keck research symposium in geology, Volume 6: Beloit, Wis., Beloit College, p. 170–172.

Lipman, P.W., 1976a, Caldera-collapse breccias in the western San Juan Mountains, Colorado: Geological Society of America Bulletin, v. 87, p. 1397–1410.

Lipman, P.W., 1976b, Geologic map of the Lake City caldera area, western San Juan Mountains, southwestern Colorado: U.S. Geological Survey Miscellaneous Investigation Series Map I–962, scale 1:48,000.

Lipman, P.W., 1984, The roots of ash flow calderas in western North America; windows into the tops of granitic batholiths: Journal of Geophysical Research B, v. 89, p. 8801–8841.

Lipman, P.W., 2000, Central San Juan caldera cluster; regional volcanic framework, *in* Bethke, P.M., and Hay, R.L., eds., Ancient Lake Creede—Its volcano-tectonic setting, history of sedimentation, and relation to mineralization in the Creede mining district: Geological Society of America Special Paper 346, p. 9–58.

Lipman, P.W., Dungan, Michael, and Bachmann, Olivier, 1997, Comagmatic granophyric granite in the Fish Canyon Tuff, Colorado—Implications for magma-chamber processes during a large ash-flow eruption: Geology, v. 25, p. 915–918.

Lipman, P.W., Fisher, W.S., Mehnert, H.H., Naeser, C.W., Luedke, R.G., and Steven, T.A., 1976, Multiple ages of mid-Tertiary mineralization and alteration in the western San Juan Mountains, Colorado: Economic Geology, v. 71, p. 571–588.

Lipman, P.W., Steven, T.A., Luedke, R.G., and Burbank, W.S., 1973, Revised volcanic history of the San Juan, Uncompahgre, Silverton, and Lake City calderas in the western San Juan Mountains, Colorado: U.S. Geological Survey Journal of Research, v. 1, p. 627–642.

Lipman, P.W., Steven, T.A., and Mehnert, H.H., 1970, Volcanic history of the San Juan mountains, Colorado, as indicated by potassium-argon dating: Geological Society of American Bulletin, v. 81, p. 2329–2351.

Luedke, R.G., and Burbank, W.S., 1961, Central vent ash-flow eruption, western San Juan Mountains, Colorado, *in* Short papers of the geologic and hydrologic sciences: U.S. Geological Survey Professional Paper 424–D, p. D94–D96.

Luedke, R.G., and Burbank, W.S., 1968, Volcanism and cauldron development in the western San Juan Mountains, Colorado, Cenozoic volcanism in the southern Rocky Mountains: Colorado School of Mines Quarterly, v. 63, p. 175–208.

Luedke, R.G., and Burbank, W.S., 2000, Geologic map of the Silverton and Howardsville quadrangles, southwestern Colorado: U.S. Geological Survey Geologic Investigation Series Map I–2681, scale 1:24,000.

Mayor, J.N., and Fisher, F.S., 1972, Middle Tertiary replacement ore bodies and associated veins in the northwest San Juan Mountains, Colorado: Economic Geology, v. 67, p. 214–230.

Mast, M.A., Verplanck, P.L., Yager, D.B., Wright, W.G., and Bove, D.J., 2000, Natural sources of metals to surface waters in the upper Animas River watershed, *in* ICARD 2000; Proceedings of the Fifth International Conference on Acid Rock Drainage, Volume 1: Society for Mining, Metallurgy, and Exploration, Inc., p. 513–522.

Molinar, Peter, and England, Philip, 1990, Late Cenozoic uplift of mountain ranges and global climate change—Chicken or egg?: Nature, v. 346, p. 29–34.

Musgrave, J.A., and Thompson, T.B., 1991, Sultan Mountain Mine, western San Juan Mountains, Colorado; a fluid inclusion and stable isotope study: Economic Geology, v. 86, p. 768–779.

Nash, J.T., 1975, Fluid inclusion studies of vein, pipe, and replacement deposits, northwestern San Juan Mountains, Colorado: Economic Geology, v. 70, no. 8, p. 1448–1462.

Nash, J.T., 2000, Geochemical studies of mines, dumps, and tailings, as sources of contamination, upper Animas River watershed, Colorado: U.S. Geological Survey Open-File Report 00–104. 1 CD-ROM.

Ratté, J.C., and Steven, T.A., 1967, Ash flows and related volcanic rocks associated with the Creede caldera, San Juan Mountains, Colorado: U.S. Geological Survey Professional Paper 524–H, p. H1–H58.

Ransome, F.L., 1901, A report on the economic geology of the Silverton quadrangle, Colorado: U.S. Geological Survey Bulletin 182, 265 p.

Ringrose, C.R., 1982, Geology, geochemistry, and stable isotope studies of a porphyry-style hydrothermal system, west Silverton district, San Juan Mountains, Colorado: Aberdeen, Scotland, University of Aberdeen Ph. D. dissertation, 257 p., 19 plates.

Smith, R.L., and Bailey, R.A., 1968, Resurgent cauldrons, *in* Coats, R.R., Hay, R.L., and Anderson, C.A., eds., Studies in volcanology—A memoir in honor of Howel Williams: Geological Society of America Memoir 116, p. 613–662.

Steven, T.A., 1975, Middle Tertiary volcanic field in the southern Rocky Mountains, *in* Curtis, B.F., ed., Cenozoic history of the southern Rocky Mountains: Geological Society of America Memoir 144, p. 75–94.

Steven, T.A., and Epis, R.C., 1968, Oligocene volcanism in south-central Colorado, *in* Epis, R.C. ed., Cenozoic volcanism in the southern Rocky Mountains: Colorado School of Mines Quarterly, v. 63, p. 241–258.

Steven, T.A., Hon, Ken, and Lanphere, M.A., 1995, Neogene geomorphic evolution of central San Juan Mountains near Creede, Colorado: U.S. Geological Survey Miscellaneous Investigations Series Map I–2504, scale 1:100,000.

Steven, T.A., and Lipman, P.W., 1976, Calderas of the San Juan volcanic field, southwestern Colorado: U.S. Geological Survey Professional Paper 958, 35 p.

Steven, T.A., Lipman, P.W., Hail, W.J., Jr., Barker, Fred, and Luedke, R.G., 1974, Geologic map of the Durango quadrangle, southwestern Colorado: U.S. Geological Survey Miscellaneous Investigations Series Map I–764, scale 1:250,000.

Steven, T.A., Schmitt, L.J., Jr., Sheridan, M.J., Williams, F.E., Gair, J.E., and Klemic, H., 1969, Mineral resources of the San Juan primitive area, Colorado: U.S. Geological Survey Bulletin 1261–F, 187 p.

Tweto, Ogden, and Sims, P.K., 1963, Precambrian ancestry of the Colorado mineral belt: Geological Society of America Bulletin, v. 74, p. 991–1014.

Varnes, D.J., 1963, Geology and ore deposits of the south Silverton mining area, San Juan County, Colorado: U.S. Geological Survey Professional Paper 378–A, 56 p.

Vincent, K.R., Church, S.E., and Fey, D.L., 1999, Geomorphological context of metal-laden sediments in the Animas River floodplain, Colorado, *in* Morganwalp, D.W., and Buxton, H.T., eds., U.S. Geological Survey Toxic Substances Hydrology Program—Proceedings of the Technical Meeting, Charleston, South Carolina, March 8–12, 1999—Volume 1, Contamination from hardrock mining: U.S. Geological Survey Water-Resources Investigations Report 99–4018–A, p. 99–106.

Yager, D.B., Mast, M.A., Verplanck, P.L., Bove, D.J., Wright, W.G., and Hageman, P.L., 2000, Natural versus mining-related water quality degradation to tributaries draining Mount Moly, Silverton, Colorado, *in* ICARD 2000; Proceedings of the Fifth International Conference on Acid Rock Drainage, Volume 1: Society for Mining, Metallurgy, and Exploration, Inc., p. 535–547.